

CONTROLLING THE LOCATION OF HYDRAULIC JUMP IN RECTANGULAR CHANNEL

A Dissertation submitted in partial fulfillment of the requirement for the
Award of degree of

MASTER OF TECHNOLOGY

IN

HYDRAULICS AND WATER RESOURCES ENGINEERING

BY

SIDDHARTH UPADHYAY
(2K15/HFE/15)

Under The Guidance of

Mr. S. ANBU KUMAR

Associate Professor
Department of Civil Engineering
Delhi Technological University
Delhi



DELHI TECHNOLOGICAL UNIVERSITY
(FORMELY DELHI COLLEGE OF ENGINEERING)

DELHI-110042

JULY 2017

CANDIDATES'S DECLARATION

I do hereby certify that the work presented is the report entitled “**CONTROLLING THE LOCATION HYDRAULIC JUMP IN RECTANGULAR CHANNEL**” in the partial fulfillment of the requirements for the award of the degree of “Master of Technology” in Hydraulics & Water Resources Engineering submitted in the Department of Civil Engineering, Delhi Technological University, is an authentic record of my own work carried out from January 2017 to July 2017 under the supervision of Mr. S. ANBU KUMAR (Associate Professor), Department of Civil engineering.

I have not submitted the matter embodied in the report for the award of any other degree or diploma.

Date: 20/07/2017

SIDDHARTH UPADHYAY
2K15/HFE/15

CERTIFICATE

This is to certify that above statement made by the candidate is correct to best of my knowledge.

Mr. S. ANBU KUMAR
(Associate Professor)
Department of Civil Engineering
Delhi Technological University

ACKNOWLEDGEMENT

I take this opportunity to express my profound gratitude and deep regards to Mr. S. ANBU KUMAR (Associate Professor, Civil Engineering Department, DTU) for his exemplary guidance, monitoring and constant encouragement throughout the course for this project work. The blessing, help and guidance given by him from time to time shall carry me a long way in life on which I am going to embark.

I would also like to thank Prof. Dr. Nirendra Dev (Head of Department, Civil Engineering Department, DTU) for extending his support and Guidance.

Professors and faculties of the department of Civil Engineering, DTU, have always extended their full co-operation and help. They have been kind enough to give their opinions on the project matter; I am deeply obliged to them. They have been a source of encouragement and have continuously been supporting me with their knowledge base, during study. Several of well wishers extended their help to me directly or indirectly and we grateful to all of them without whom it would have been impossible for me to carry on my work.

Abstract

As per the report of International Commission on Large Dams (ICOLD) demonstrate that over 20% of dam mishaps happened because of poor arrangement of energy dissipation. At present, energy dissipators are intended for 'design discharge' of spillway. In this manner there is a need to build up a proper plan to perform expected function of energy dispersal even at lower discharge. Present work concentrated on hydraulic jump type energy dissipators. It is found that in majority of failure of dam, the jump position is not specified – i.e. jump is either swept up or drowned. So it is required to manage the position of hydraulic jump so that the front of jump is positioned near toe of spillway or sluice gate to get clear jump.

A clear hydraulic jump occur inside stilling basic , once the ideal post jump depth as per Belanger momentum equation is available on apron. To restrain the formation of clear hydraulic jump within basin, a stepped weir at the end of apron is suggested. A mathematical method is developed to design the weir geometry which will form desired post jump depth corresponding to any discharge between design discharge and 20% of the design discharge and the given range of tail water submergence. Experiments in ansys fluent demonstrate that, for horizontal aprons, a designed weir section, designed for a specific range of tail water submergence, restricted the hydraulic jump to its desired location for different discharges. The correlation coefficients for ansys fluent studies with experimental value for horizontal apron ranged between 0.989 to 0.99. This technique is applicable for 'inflow Froude number ≥ 4.5 '. The methodology would provide promising results in real life projects.

CONTENTS

Candidate declaration	ii
Certificate	ii
Acknowledge	iii
Abstract	iv
List of Figures	vii
List of Tables	ix
Nomenclature	x
Chapter 1	
Introduction	01
Introduction	01
Chapter 2	
Literature review	04
2.1 Energy Dissipators	04
2.2 Types of energy dissipators	04
2.3 Factors affecting design of energy dissipators	05
2.4 Effects of inadequate energy dissipation	07
2.5 Guidelines of USBR Monograph 25	09
2.6 Hydraulic Jump as an Energy Dissipator– An Overview	09
2.7 Control of Hydraulic Jump by Sharp Crested Weir	10
2.8 Hydraulic Jump on Sloping Apron	10
2.9 Importance of Location Control	14
2.10 Efforts made so far to achieve location control	15
Chapter 3	
Methodology	16
3.1 Proposed Methodology	16
3.2 Governing Factors	20
3.3 Development of mathematical procedure	20
3.4 Determination of Appropriate C_d	25
3.5 Determination of Appropriate C_{dm}	29

Chapter 4	
CFD Studies and Results	33
4.1 Computational Fluid Dynamics	33
4.2 Numerical modeling	33
4.3 CFD Model Setup	34
4.4 Preprocessing	35
4.5 Case study of Pawana Dam	49
4.6 Results and Discussions	54
Chapter 5	
Conclusions	56
5.1 Practical Applications	56
5.2 Limitations	57
5.3 Future Scope	57
References	58

LIST OF FIGURE

1.1	Definition sketch of hydraulic jump in rectangular channel	03
2.1	Damage to stilling basin floor of SSP	08
2.2	View of Dislodge RCC panel in bhama askhed Dam	09
2.3	Types of sloping jump A,B,C and D	11
2.4	Comparison of TWRC,FJHC and FRJHC	15
3.1	Definition sketch of hydraulic jump in rectangular channel	16
3.2	Classification of tail water condition for design of energy dissipater	17
3.3	Position of hydraulic jump at design and lower discharge for end weir	
	Designed for design discharge condition	20
3.4	Design of rectangular stepped weir	22
3.5	Schematic of zigzag geometry of stepped weir	24
3.6	Definition sketch of geometry of rectangular stepped weir	25
4.1	Experimental setup	35
4.2	Schematic of problem setup prepared in gambit	36
4.3	View of stepped weir section resting on channel bottom	40
4.4	Flume section with stepped weir	41
4.5	Flume in meshed form	41
4.6	Vertical view of stepped weir	42
4.7	Flow inlet section in flume	42
4.8	Flow outlet section in flume	43
4.9	Hydraulic jump at discharge ($Q = 0.0020 \text{ m}^3/\text{s}$)	43
4.10	Hydraulic jump at discharge ($Q = 0.0052 \text{ m}^3/\text{s}$)	44
4.11	Hydraulic jump at discharge ($Q = 0.0068 \text{ m}^3/\text{s}$)	44
4.12	Hydraulic jump at discharge ($Q = 0.0084 \text{ m}^3/\text{s}$)	45
4.13	Hydraulic jump at discharge ($Q = 0.0092 \text{ m}^3/\text{s}$)	46
4.14	Hydraulic jump at discharge ($Q = 0.0100 \text{ m}^3/\text{s}$)	46
4.15	Comparison of experimental and fluent jump height curve ($C_d=0.50$)	47
4.16	Comparison of experimental and fluent jump height curve ($C_d=0.55$)	48

4.17	Comparison of experimental and fluent jump height curve ($C_d=0.60$)	48
4.18	Schematic problem setup for Pawana dam spillway in gambit	49
4.19	Inlet section of flume model of Pawana dam spillway	50
4.20	outlet section of flume model of Pawana dam spillway	50
4.21	Meshed form of flume model of Pawana dam spillway	51
4.22	Comparison of experimental and fluent jump height curve for designed Weir	52
4.23	Comparison of experimental and fluent jump height curve for existing Broad crested weir	53

LIST OF TABLES

3.1	Calculations of Y_2 by two methods	24
3.2 (a)	Output of mathematical procedure data ($C_d=0.6$)	27
3.2 (b)	Output of mathematical procedure data ($C_d=0.65$)	28
3.2 (c)	Output of mathematical procedure data ($C_d=0.63$)	29
3.3	Comparison of submergence flow coefficient K and K_s	31
4.1	Comparison of post jump depth for horizontal apron for ($C_{dm}=0.6$)	38
4.2	Comparison of post jump depth for horizontal apron for ($C_{dm}=0.55$)	39
4.3	Comparison of post jump depth for horizontal apron for ($C_d=0.5$)	39
4.4	Comparison of post jump depth for sloping apron for Pawana dam Experiments and fluent for designed weir	52
4.5	Comparison of post jump depth for sloping apron for Pawana damn for Existing weir	53

NOMENCLATURE

B	=	Width of rectangular channel
B	=	Width of step of rectangular stepped weir
C_d	=	Coefficient of discharge for free weir
C_{dm}	=	Modified coefficient of discharge
Fr_1	=	Supercritical Froude number
Fr_2	=	Subcritical Froude number
H	=	Head on upstream of the sluice gate or spillway
H_j	=	Height of jump
H	=	Head over weir crest
K	=	Submerged flow coefficient
k_s	=	Submerged flow coefficient for stepped weir
L_j	=	Length of jump
Q	=	Discharge
S_r	=	submergence ratio
v_1	=	Supercritical velocity (neglecting losses)
v_2	=	Subcritical velocity (neglecting losses)
y'	=	Height of weir crest from the channel bed
Y_1	=	Pre jump depth
Y_2	=	Post jump depth or sequent depth

Chapter 1

Introduction

Hydraulic jump type energy dissipators are widely accepted methods of energy dissipation while designing the hydraulic structures like dams, weirs and barrages. They are popular for their simplicity and efficiency, but have certain limitations when there is variation in discharge conditions. The energy dissipators satisfactorily function at design discharge condition. But in case of varying discharge conditions they are not efficient as the location of hydraulic jump tends to shift on apron. This would result in percentage reduction in energy dissipation and in turn damage hydraulic structures and adversely affect tail channel conditions. Hence with an aim to resolve this problem, an attempt has been made to create a forced hydraulic jump at desired location for varying discharge conditions. A new technique is developed and studied in depth for designing hydraulic jump type energy dissipators with reference to tail water deficiency.

The forced hydraulic jumps are used for energy dissipation in stilling basins. It is a jump formed with the assistance of baffles and/or sill with or without sub critical tail water. In the recent past the contribution in this regard is due to Rajaratnam (1971, 1991, 1995, 2002), Bhowmik (1975), Hager (1989, 1992), Chaudhry (1991, 1995) et al. A hydraulic jump forms when a high velocity supercritical flow suddenly transforms into a relatively low velocity subcritical flow, accompanied by formation of eddies, rollers and turbulence along with air entrainment. Ultimately the energy is dissipated in the form of heat. The formation of hydraulic jump at the foot of spillway or under the sluice gate acts as an energy dissipator. The maximum energy dissipation occurs when a clear hydraulic jump forms at the section where the prejump depth is minimum. This is because when pre jump depth is minimum, as per Belanger equation (Vittal and Al-Garni 1992), its sequent depth i.e. post jump depth is maximum and thus the ratio of post jump depth to prejump depth is maximum and hence the initial Froude number is maximum. As energy dissipation is directly proportional to initial Froude number, for the given inflow condition the energy dissipation is maximum. It is well known that the length of the apron depends upon the length and location of the jump (for design discharge condition) which in turn depends on the pre jump depth (y_1) and the relative magnitudes of post jump depth

(y_2) and tail water depth (y_t) (Rajaratnam and Subramanya 1966; Jeppson 1970). As shown in Fig. 1.1, the pre jump depth (y_1) which is in supercritical state and post jump depth (y_2) which is in subcritical state are called as sequent depths and the tail water depth (y_t) is the depth of water on downstream of the weir. In a rectangular channel with horizontal slope, hydraulic jump forms at a location where these sequent depths satisfy Belanger equation.

The sequent depths are referred corresponding to the section at vena contracta as the ideal location of jump is at vena contracta of supercritical flow (Chow 1959). As the term vena contracta is normally used in connection with the gated flow, in case of spillway flows the vena contracta would be referred to a section where the prejump depth (y_1) is minimum. In case of tail water deficiency condition, the tail water rating curve lies below the jump height curve for all the discharges. Due to this the hydraulic jump may partially or fully sweep out of the basin and is not advisable as it would result in damage to stilling basin, tail channel and other downstream structures (Tung and Mays 1982; Moharami et al 2000). Thus it becomes very much significant to have the location of hydraulic jump in a stipulated zone (i.e. on apron), to successfully accomplish the task of energy dissipation (Rouse et al 1958). For this purpose the depth of water on the apron may be artificially raised to such a magnitude that it becomes sequent to the pre jump depth at vena contracta and form the jump at vena contracta (Leutheusser and Kartha 1972; Ohtsu et al 1991). That means by forming forced post jump depths on apron, the efforts can be made to match them with post jump depths given by Belanger equation for all the discharges (Vittal and Al-Garni 1992). This can be achieved by introducing an impediment in the form of weir at the end of the apron. (Pillai et al 1989; Gharangik and Chaudhry 1991; Rahman and Chaudhry 1995).

In practice the rectangular broad crested weirs are considered for this purpose (Achour and Debabeche 2003). The weir with its height designed for design discharge condition, is not suitable under field conditions where discharges would vary and generally less than design discharge. Therefore to address this problem an attempt has been made to design an end weir geometry which would assure formation of clear

jump at vena contracta for the design discharge as well as for the lower discharges. The main focus of the present study is to develop a mathematical procedure and computational technique to design an appropriate end weir to restrict location of hydraulic jump near sluice gate or toe of spillway for varying discharge conditions. The study is carried out in two stages. In the first stage weir section is designed considering free flow over weir crest. In the second stage three weir sections corresponding to three different tail water submergence conditions are designed and tested in flume to confirm the location of jump at desired place. In order to generalize the application, sloping apron is considered. The mathematical procedure is then applied to hydraulic jump on sloping apron. In this case three different slopes and corresponding to each slope, three different tail water submergence conditions are considered. For each of the nine cases, nine weir sections are designed and tested in flume to confirm the location of jump at desired place.

A model study of single span of an existing spillway energy dissipator is carried out in laboratory to check the applicability of the weir. A CFD technique (fluent) is used to support the experimental findings numerically. A numerical model fluent is first validated with the help of results obtained through laboratory experiments. Finally, a pilot scale physical model study is carried out by using data of existing dam in India. The weir designed for this purpose is fabricated after testing its performance on fluent. Thus a new design of stilling basin in the form of horizontal apron with a rectangular broad crested stepped weir is proposed. The details of the study are reported here in.

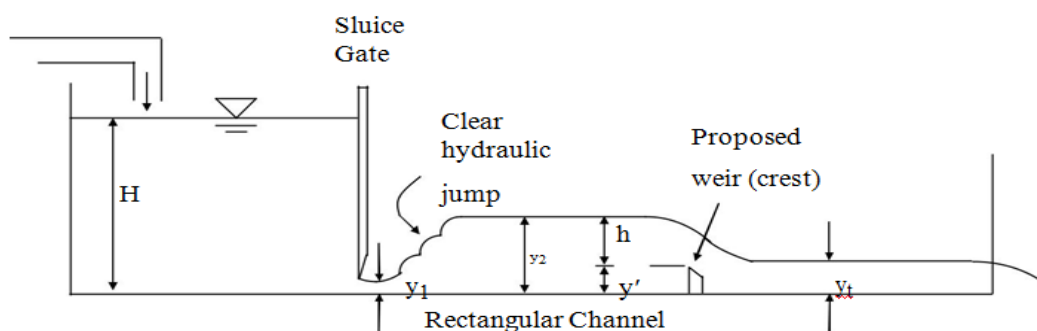


Fig 1.1 Definition sketch of hydraulic jump in a rectangular channel

CHAPTER 2

LITERATURE REVIEW

2.1 Energy Dissipators

When spillway flows fall from reservoir pool level to downstream river level, a large part of static head (total head reduces by losses) is converted into kinetic energy. This energy manifests itself in the form of high velocities which if impeded, results in large pressures. On the other hand, if the high energy of flow is not dissipated, serious erosion to stream bed and damage to hydraulic structures may be caused. The device used to protect the river or tail channel and the hydraulic structures on downstream, is called as energy dissipator. The function of energy dissipator is to absorb high energy of spillway flows and discharge these flows to the downstream water course, without causing serious scour or erosion of the toe of the dam/spillway or damage to adjacent structures (IS 4997 1968).

2.2 Types of energy dissipators

IS 4997 (1968) gives classification of different types of energy dissipators. Normally a hydraulic jump type stilling basins and bucket type energy dissipators are used depending upon conditions of downstream tail water. Although in case of projects where fall is greater than 15 m or discharge intensity is more than $30 \text{ m}^3/\text{s}/\text{m}$ or for possible asymmetry of flow, it is recommended that performance of energy dissipation arrangement shall be tested on model.

2.3 Factors affecting design of energy dissipators

- i) Nature of foundations (geological conditions)
- ii) Magnitude of floods and their recurrence
- iii) Velocity of flow
- iv) Tail water rating curve (i.e. depth-discharge relationship of the downstream water course at the site of the structure).

i) Nature of Foundation

(**Khatsuria 2005**) explains that the foundation of dam, spillway and that of tail channel should be of sound rock and should be watertight. The cracks and interconnected passages present in the rock may lead to uplift pressures. The static and dynamic uplift due to tail water may cause damage to stilling basin floor .

ii) Magnitude of floods and their recurrence

The estimation of spillway design flood or the inflow design flood is an exercise involving diverse disciplines of hydrology, meteorology, statistics and probability. Several countries have formed their own guidelines or regulations for determination of spillway design flood. In India mostly US guidelines are followed.

(**Khatsuria 2005**) Generally large dams (storage capacity > 51.7 MCM) are designed for PMF, intermediate dams/barrages (storage capacity < 51.7 MCM) for SPF/PMF and small dams for floods of return period of 100 years to SPF.

Bowers and Toso 1988 studies finds that Once the spillway design flood is finalized, accordingly spillways are designed. During operations, depending upon the situation, spillways have to pass discharges lower than the design discharge. It may vary from 20% to 100% of design discharge. It should be noted that the damage to Karnafuli dam's spillway and stilling basin (Bangladesh) occurred at 20% of design discharge of spillway.

iii) Velocity of flow

The velocity of flow depends on head or energy on upstream. In other words it is the elevation difference between the head race and the top of apron (H). Higher the energy on upstream, at toe of spillway, higher will be the supercritical velocity of flow and lower will be the depth of flow. This means the Froude number F_{r1} will also be higher. Now higher the inflow Froude number, higher will be the length of hydraulic jump and larger will be the length of stilling basin. Hence on the grounds of economy, instead of hydraulic jump type one may go in for other types of energy dissipator

which are comparatively economical (provided the foundation conditions are suitable). Secondly higher velocity may lead to cavitation and the subsequent damage to stilling basin, appurtenances, tail channel and ultimately the spillway or the dam as a whole. Not only high velocities, but low velocities with lot of fluctuations give birth to fluctuating pressures and prove to be dangerous.

(Cassidy 1990) The floor blocks of Pit 7 dam in Northern California were damaged on account of the swept up hydraulic jump and exposure of blocks to supercritical velocities.

(Peterka 1984) USBR Monograph 25 gives formula to calculate supercritical velocities at the foot of spillway.

iv) Tail water rating curve (i.e. depth-discharge relationship of the downstream water course at the site of the structure)

The last factor, i.e. tail water rating curve, is the most important of all the factors. A thorough knowledge of its implications on the design of energy dissipation arrangements is a pre-requisite for the design of the most efficient and at the same time cheapest type of structure to serve the purpose. The accuracy of prediction of the prototype performance from the model studies or from theoretical calculations leading to the design of energy dissipator, depends entirely on the accuracy of the data related to depth-discharge relationship at the particular site, where the structure is proposed to be constructed.

The simplest kind of device to dissipate energy of the high velocity flow is to enable the formation of hydraulic jump. If the conditions are such that the jump would form for all discharges on a horizontal floor at the stream bed level, then a simple paving on the stream bed extending from the dam to the downstream end of the jump would serve the purpose.

A tail water rating curve, for the regime of the river below spillway is fixed by the natural conditions along the stream and is generally not changed by the spillway design or by release characteristics. However retrogression / aggradation of the river below the dam which will affect the ultimate stage discharge conditions must be taken into account while selecting the type of energy dissipating arrangements. Usually where river flows which approach the maximum design discharge have never occurred, an estimate of the tail water rating curve must either be extrapolated from known conditions or computed on the basis of assumed or empirical criteria.

2.4 Effects of inadequate energy dissipation

(Chaudhry 2008) mentioned that more than 20% of dam accidents occurred due to poor provision of energy dissipation arrangements. Various case studies related to damages of spillways and stilling basins and tail channel erosion are reported all over the world. These studies have revealed the importance of adequate energy dissipating arrangements. Following are some of the illustrations of damages due to inadequate energy dissipation.

2.4.1 Sardar Sarovar Project

Sardar Sarovar Project (SSP) is one of the major projects in India. In the year 1999 it is reported that during a flood in monsoon season, 10,000 m³ of concrete was washed out due to flood flows. The design discharge of spillway is 87,000 m³/s. The flood was even lesser than 50% of the design discharge. The approximate cost of concrete that washed out was Rs. 3 crore. Also it was mentioned that the damage of varying magnitude occurs almost every year.

Khaturia (2005) has given the technical analysis of the damage and is briefly discussed below. Flow situations downstream of partly constructed spillway are often unacceptable and conducive to harm. When dissimilar monoliths are kept at various different elevations instead of at uniform level for the entire spillway, unequal discharge distribution happens. Floors of hydraulic jump stilling basins are mainly vulnerable to damage due to horizontal eddies constructing in the downstream. Such eddies pickup loose material from downstream, bring it inside the basin, and cause abrasion damage to the concrete floor, generally known as roll-mill action. The damage sometimes is so extensive as to expose the reinforcement steel of the apron floor. Fig. 2.1 shows view of damaged stilling basin floor of a dam as a result of the abrasion caused due to material that was brought in by the return eddies during a construction stage. This, probably, cannot be prevented in ordinary situations. A prevention adopted at the Sardar Sarovar Dam, was to provide a number of low height divide walls in the basin.

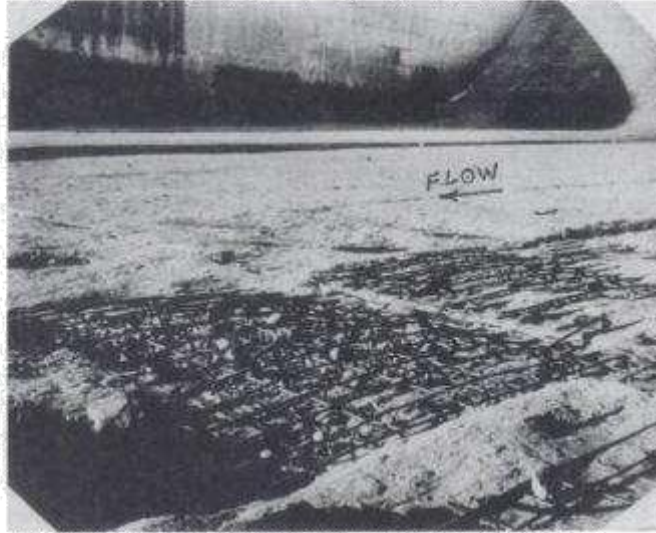


Fig. 2.1 Damage to stilling basin floor of SSP

2.4.2 Bhama Askhed Dam (India)

Hinge G. A., Balkrishna S., Khare K.C. (2010) studies on Bhama Askhed Dam EDA (India), in the year 2005, showed that flood damages have occurred. 12 out of 35 RCC panels (of size 11m x 7m x 0.3m thick and weighing 55 Tons each and with 5-anchor bars of 25mm diameter) were dislodged from their location and few of them were thrown away outside the basin. It will be clear from photographs shown in Fig 2.2.



Fig. 2.2 View of dislodged RCC panels in Bhama Askhed dam EDA

2.5 Guidelines of USBR Monograph 25

USBR Monograph-25 “Hydraulic Design of Stilling Basins and Energy Dissipators”, by A. J. Peterka, specifies the designs of stilling basins, energy dissipators of several types and related appurtenances. common design rules are presented so that the essential dimensions for a specific structure may be effortlessly and quickly determined and the values can be selected (checked by others) without the need for exceptional judgment or extensive previous experience. It deals with the hydraulic phenomenon of energy dissipation in hydraulic structures. As already mentioned, the focus is on currents with comparatively high rate of energy dissipation, i.e. flows in which significant energy is dissipated in a limited amount of space.

Energy dissipaters are used in pressurized flows as well as in open channel flows. They provide a transition between high and low hydraulic energy. Three such transitions can be distinguished:

- One pressure conduit to another,
- A pressure conduit to a channel,
- One channel to another channel.

This monograph includes primarily those energy dissipators that think either pressure conduits to channels or one channel to another. The other types comprise the rich variety represented by throttles, pressure valves, mixing tubes, etc which are not dealt in monograph.

2.6 Hydraulic Jump as an Energy Dissipator– An Overview

Chow (1959) has given a chronological development of hydraulic jump theory. The theory of jump developed in early days is for horizontal or slightly inclined channels in which the weight of water in the jump has little effect upon the jump behavior and hence is ignored in the analysis. The results thus obtained, however, can be applied to most channels encountered in engineering problems. For channels of large slope, the weight effect of water in the jump become pronounced and needs to be included in the analysis. The hydraulic jump is also known as standing wave.

2.7 Control of Hydraulic Jump by Sharp Crested Weir

Forster and Skrinde, the hydraulic jump can be controlled by sills of various designs such as sharp crested weir, broad crested weir, abrupt rise or abrupt drop in channel floor (**Chow 1959**).

(**Hager and Li 1992**) The function of a sill is to ensure formation of jump and to control its position under all probable operating conditions .

(**Narayanan and Schizas 1980**) At high submergence, the drag force on sill essentially depends on the ratio of sill height to prejump depth. The exact position of the jump, as controlled by the sill, however cannot be determined analytically. It is presumed by Forster and Skrinde that tail water level does not affect y_2 . That means the tail water submergence effect has been neglected.

2.8 Hydraulic Jump on Sloping Apron

(**Subramanya 1986**) Experimentation with hydraulic jumps created in sloping channels were carried out by many researchers to find out the kind of properties that are same as those relating to jumps in horizontal channels. The one dimensional momentum principle for the sequent depth ratio cannot be useful because the component of weight of jump ($W\sin\theta$) is not known a priori. This is because $W\sin\theta$ considers the length and profile of the jump, information about which can be obtained only through experimental study. As such, even though many efforts have been made to obtain the sequent depth ratio through the momentum equation, no satisfactory general solution is available so far.

2.8.1 Types of hydraulic jumps on slope

Kindsvater classified the jumps in 1944 according to their toe position relative to the bottom kink (Hager 1992) as A, B, C, and D as shown in Fig. 2.3. Hydraulic jumps in sloping channels may occur in various forms.

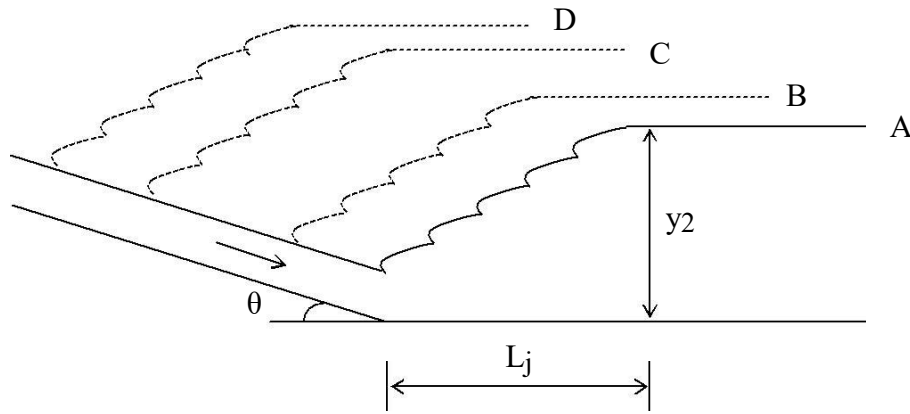


Fig. 2.3 Types of Sloping Jumps - A, B, C and D

A-type jump is nothing but a jump on horizontal apron. As per Chow (1959), B, C and D are known as drowned out jumps and are the common forms which usually appear simply as jets of water plunging into a downstream pool below a steep slope. For practical purposes, it is believed that the solutions for the typical form of hydraulic jump on sloping apron are applicable to B, C and D-type of jumps. A and B-type of jumps mostly occur with steep slope channel (i.e. downstream face of spillway) followed by horizontal or nearly horizontal apron. C and D-type of jumps occur on relatively flat or small sloping channels.

Gunal and Narayanan (1996) have studied the internal structure of hydraulic jumps wholly formed on channels of small slopes ranging from 0 to 0.1.

Ohtsu and Yasuda (1991) studied D and B-type jumps and have proposed practical equations for the sequent depths and the length of jumps.

Hager (1989) investigated B-jump in sloping channel and concluded that the jump efficiency is maximum for the classical hydraulic jump.

Alhamid (2004) studied the jump characteristics on sloping basins and confirmed that the sequent depth ratio is proportional to the bed slope.

The Froude number of flow in rectangular channel with large θ is given by

$$F_{1S} = \frac{V_1}{\sqrt{g \cdot y_1 \cdot \cos \theta}} \quad (2.1)$$

2.8.2 Characteristics of Jump on a Sloping Floor

Extensive experiments have been conducted by the United States Bureau of Reclamation resulting in useful information on jumps on a sloping floor. Based on the USBR study following significant characters of sloping-floor jumps can be noted

i) Sequent depth y_{2S}

Defining y_2 = equivalent depth corresponding to y_1 in a horizontal floor jump

$$Y_2 = \frac{Y_1}{2} \left(-1 + \sqrt{1 + 8 F_{r1}^2} \right) \quad (2.2)$$

The sequent depth y_2 is found to be related to y_{2S} as

$$\frac{y_{2S}}{y_2} = f(\theta) \quad (2.3)$$

The variation of y_{2S} / y_2 with $\tan\theta$ is given by Subramanya (1986). By definition $y_{2S} / y_2 = 1$ when $\tan\theta = 0$ and it increases with the slope of the channel having typical values of 1.4 and 2.7 at $\tan\theta = 0.10$ and 0.30 respectively. Thus the sloping jumps require more sequent depths than the corresponding horizontal-floor jumps.

The best fit line for the variation of y_{2S} / y_2 with $\tan\theta$ can be expressed as

$$\frac{y_{2S}}{y_2} = 1.0071 \cdot e^{(3.2386 \tan \theta)} \quad (2.4)$$

ii) Length of sloping jump L_j

The length of sloping jump L_j was defined in the USBR study as the horizontal distance between the commencement of the jump and a point on the subcritical flow region where the streamlines separate from the floor or to a point on the level water surface immediately downstream of the roller, whichever is longer. The length of the jump on a sloping floor is longer than the corresponding length of jump on a horizontal floor. The variation of L_j / y_2 with F_1 for any θ is similar to the variation for $\theta = 0$. In the range of $4.0 < F_1 < 13$, L_j / y_2 is essentially independent of F_1 and is a function of θ only. The variation can be approximately expressed as

$$L_j / y_2 = 6.1 + 4.0 \tan\theta \dots \dots \dots \text{in the range of } 4.5 < F_1 < 13.0 \quad (2.5)$$

Elevatorski's analysis of the USBR data indicates that the jump length can be expressed as

$$L_j = m_s (y_2 - y_1) \quad (2.6)$$

In which $m_s = f(\theta)$. The variation of m_s with $\tan\theta$ is given by **Subramanya (1986)**. It may be seen that for $m_s = 6.9$, $\tan\theta = 0$ and it decreases with an increase in the value of the channel slope.

iii) Energy loss E_{Ls}

Knowing the sequent depths y_2 and y_1 and the length of the sloping channel, it is found that the relative energy loss E/E_1 decreases with an increase in the value of θ , being the highest at $\tan\theta = 0$.

In short, as compared to jump on horizontal floor, the sloping jump requires larger post jump depth and larger length of stilling basin. Also the relative energy loss in the sloping jump is less than the corresponding horizontal jump. It should be noted that, in a sloping jump, rather than Froude number, the angle θ plays a vital role.

2.8.3 Other Applications of Hydraulic Jump

The important practical application of hydraulic jump is that it is a most popular energy dissipating device. But apart from this, it is also used for various other purposes mentioned below.

1. Hydraulic jump is used to increase the water depth on the apron and thus to compensate the uplift pressure.
2. It is used to raise water level in irrigation canals to increase the command area.
3. It is used for thorough mixing of chemicals and for aeration in water treatment plants.
4. It is used for aeration and dechlorination of waste water.
5. It is used to remove air pockets from water supply pipes.
6. It is used for heat energy dissipation of hot water in thermal power plants before it joins the natural water body.

2.9.1 Importance of Location Control

The maximum energy dissipation occurs when a clear hydraulic jump forms at vena contracta of supercritical flow near the sluice gate or the section where prejump depth is minimum near the toe of spillway. The magnitude of energy dissipation for this case is maximum because of following reasons.

1. The ratio y_2 / y_1 is maximum.
2. Therefore Froude number F_{r1} is maximum
3. As energy dissipated in the jump E is proportional to F_{r1} , the energy dissipation is maximum.

Therefore, we have to maximize the ratio of sequent depths y_2 / y_1 . Theoretically this can be done by decreasing y_1 or increasing y_2 or by changing both simultaneously. Out of the two parameters – y_2 and y_1 , being a prejump depth, y_1 cannot be changed so easily. Hence the only alternative to maximize energy dissipation is to increase y_2 upto its optimum limit, that is, the ideal post jump depth given by Belanger equation.

2.9.2 Factors Affecting Location of Jump

It is clear that the post jump depth on apron is required to be adjusted to locate the jump near toe of spillway or sluice gate. Further it should be equal to the ideal post jump depth given by Belanger equation. Therefore, for appropriate location of jump over a wide range of discharge, it is necessary to generate the required post jump depth on horizontal apron which is influenced by various factors. These factors include the range of discharge and Froude number F_{r1} (i.e. prejump depth y_1 and head over spillway), the width of stilling basin and tail water depth y_t . In case of hydraulic jump type stilling basin, at basin end, normally there is end sill or dentated sill or rectangular end weir. When there is free flow over weir, the tail water level does not affect post jump depth on apron. But in most of the cases the crest of the sill / weir is submerged, and it has direct impact on the magnitude of post jump depth on apron. At present, no energy dissipator design considers tail water depth as input parameter over a wide range of discharge conditions. The tail water submergence varies along with variation of discharge.

2.10 Efforts made so far to achieve location control

Vittal and Al-Garni (1992) made notable contribution in this regard to attempt to modify USBR type III stilling basin with an aim to make it work efficiently even for discharges lower than the design discharge of spillway. According to present practice, all energy dissipators are conventionally designed for a single discharge .

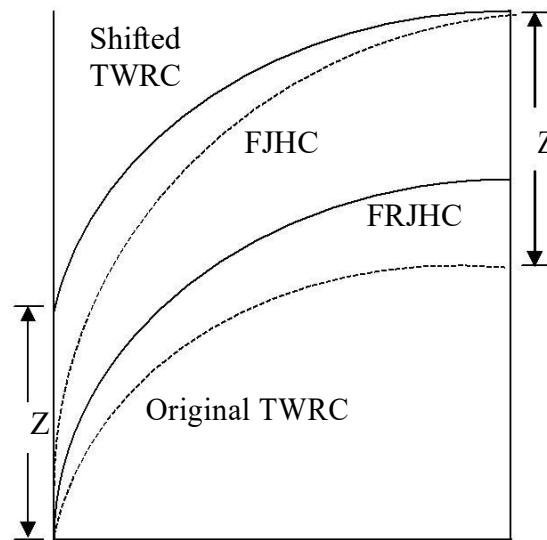


Fig. 2.4 Comparison of TWRC, FJHC (river bed level) and FRJHC (conventional design)

As a first step in design, basin floor level is lowered by Z , just enough to balance the deficiency of tail water at the design discharge with the result that the TWRC shifts upwards so as to intersect the FJHC at design discharge but create tail water excess at all lower discharges. As the second step, standard shaped appurtenances are introduced in the basin with the result that the FJHC swings clockwise into forced jump height curve (FRJHC), creating a further tail water excess at all discharges including the design discharge. The shifted TWRC and the swung FRJHC both are shown with solid lines. While the conventional design ensures non-occurrence of tail water deficit and hence eliminates swept up jump, it results in severe drowned jump at all discharges.

Chapter 3

Design Philosophy

3.1 Proposed Methodology

To achieve appropriate position of hydraulic jump in rectangular channel of width B , it is essential to consider input parameters which govern position of jump. Fig 3.1(a) demonstrates definition sketch of hydraulic jump in rectangular channel with horizontal slope.

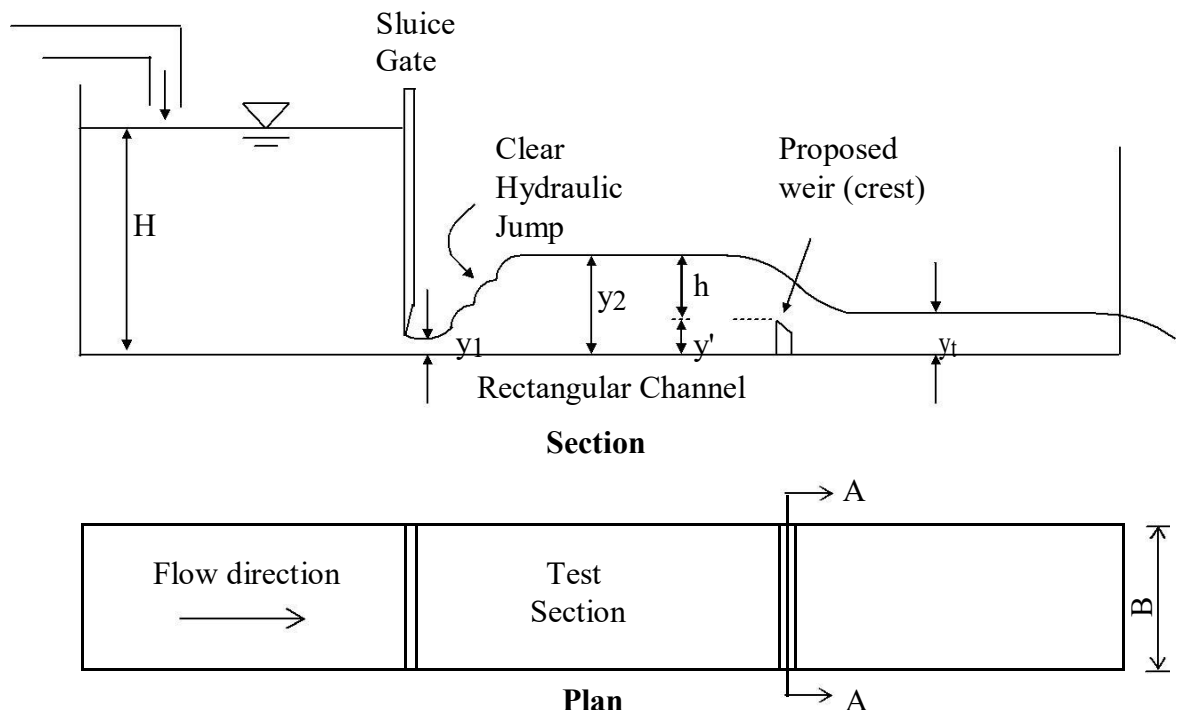


Fig. 3.1 Definition sketch of hydraulic jump in rectangular channel

Factors affecting hydraulic jump are total head on upstream of sluice gate (H), prejump depth (y_1), post jump depth (y_2), crest height of weir (y'), head over weir crest (h) and tail water depth (y_t). Another non dimensional important parameter that governs hydraulic jump phenomenon is supercritical Froude number F_{r1} .

Fig. 3.2 shows discharge Q on X-axis and post jump depth (y_2) and tail water depth (y_t) on Y-axis to form two curves - 'jump height curve' (JHC) and 'tail water rating curve' (TWRC) respectively.

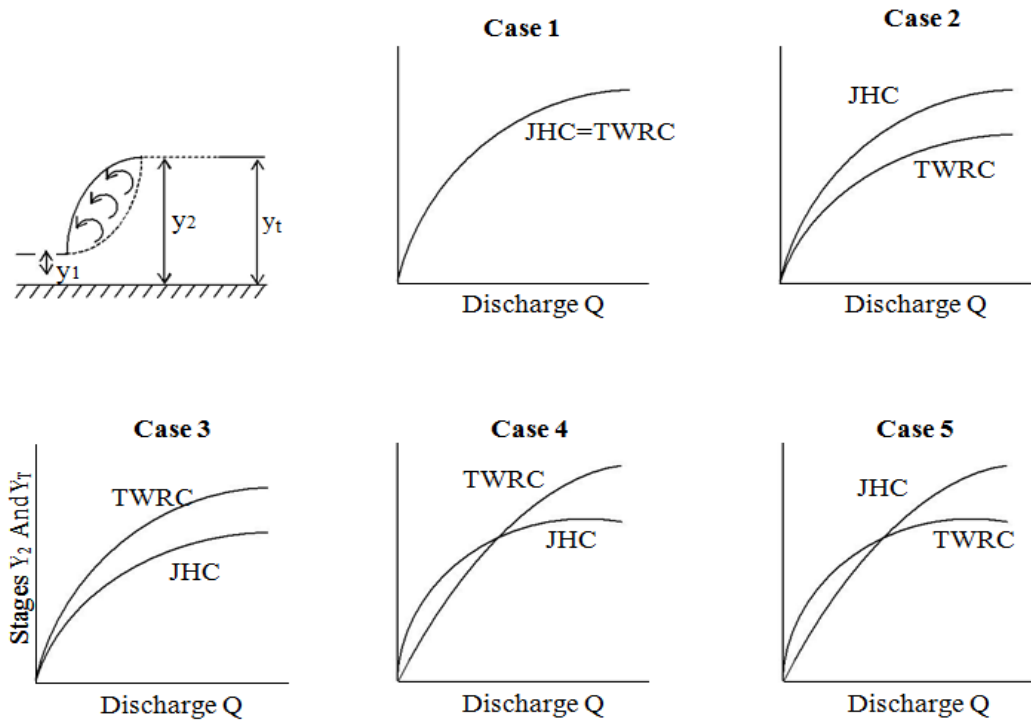


Fig. 3.2 Classification of tail water conditions for the design of energy dissipator

Depending upon the relative magnitudes of y_2 and y_t at various discharges, five different cases would arise (Chow 1959). The vertical distance between JHC and TWRC represents the difference between y_2 and y_t for a particular discharge. When this difference is zero, i.e. $y_t = y_2$, the hydraulic jump forms at vena contracta of the supercritical flow. If this condition is achieved for all the discharges, it becomes an ideal condition (Case -1) that ensures formation of clear hydraulic jump at vena contracta for all the discharges. This situation does not require any appurtenances in the stilling basin and only horizontal apron with its top at river bed elevation would suffice the requirement. But such conditions are of rare occurrence in practice.

In most of the cases on field, the tail water depths are either on higher side or lower side. Sometimes these are partly on higher side and partly on lower side and vice versa over the whole range of discharge. Hence it directly affects the position of hydraulic jump on apron. If $y_t < y_2$ (Case -2), then hydraulic jump sweeps out of the

basin and the corresponding jump is referred to as swept up jump. In this case the jump may form far away from toe of spillway but remain partly on apron or it may completely sweep out and form in the downstream channel entirely away from the stilling basin. If $y_t > y_2$ (Case -3), then the hydraulic jump rides on sloping spillway surface and the corresponding jump is referred to as submerged or drowned jump. In this case a high velocity flow extends on apron upto a large distance and it may cause scouring of the apron. Sometimes it may extend even upto the end sill. Secondly, in the drowned jump, large scale pressure fluctuations are observed (Bower and Toso, 1988). In case-4, $y_t < y_2$ for lower discharges and for the remaining discharges $y_t > y_2$, whereas in case-5 $y_t > y_2$ for lower discharges and for the remaining discharges $y_t < y_2$.

Present study focuses attention on the tail water deficiency condition (Case-2). It is also partly applicable to case-4 where there is tail water deficiency at lower discharges. Case-2 shows that over a complete range of discharge, the tail water depth is lower than the post jump depth. The difference between these two depths goes on increasing with increasing discharge. Accordingly the position of jump shifts on apron and the toe of jump moves farther and farther away from the desired position i.e. toe of spillway or sluice gate. As the jump moves away from its desired location, there is proportionate reduction in the dissipation of energy.

The tail water deficiency conditions encounter mainly on spillways located on flanks. As the tail channel is intended to convey flood water to the original river channel, it has large elevation difference in short distance, hence it is relatively steeper. This tends to produce higher velocities and subsequent lower flow depths in the tail channel. Hence due to non availability of sufficient tail water depths for formation of jump, the jump has a tendency to sweep out. As the swept up jump is rather harmful than the drowned jump, it is preferred to have a hydraulic jump type stilling basin in the form of depressed horizontal apron and an end sill which produces drowned jumps at low discharges. Another solution is to have horizontal apron – may be at river bed level or slightly depressed with a rectangular broad crested weir located at the end of the apron, generally referred as ‘end weir’. As drowned jumps dissipate less energy than the clear jumps, the residual energy carried by the water in the tail channel after it enters the tail channel is comparatively large.

In this study it is presumed that the apron elevation on just upstream of the end weir and elevation of the channel floor just downstream of the end weir are same. In some of the cases only the apron elevation is lowered to match the y_2 levels with that of y_t levels. But an additional excavation cost is also involved in lowering the apron elevation. With an aim to provide a generic solution to the problem of tail water deficiency, it is proposed to design an end weir geometry which will cater to wide range of discharge by taking the cognizance of corresponding range of tail water submergence. By way of the proposed solution an attempt would be made to overcome tail water deficiency condition to attain ideal condition. It is known that a single rectangular suppressed weir of particular height is able to cater to only single particular discharge. If a weir designed for low discharge is exposed to higher discharge, the jump will sweep out. If a weir designed for high discharge is exposed to lower discharge, a drowned jump will be formed as shown in Fig. 3.3. It means practically, under constant head, every particular discharge demands, a particular height of end weir which will be proportional to that discharge. On the other hand, if a contracted weir is designed, it results into lowering of crest height and for every particular discharge a particular width of weir is obtained which is inversely proportional to discharge.

In short, if width is kept constant, crest heights vary and if crest height is kept constant then widths vary. To achieve the aim of the study, it is necessary to design single end weir geometry in such a fashion that it will provide effect of all such individual weir heights or widths. It is therefore thought that a rectangular stepped weir may serve this purpose. On fields, normally end weirs are provided in form of broad crested weirs which are gravity structures. In other small projects they can be provided in the form of sharp crested weirs. As broad crested weirs have high modular limit (0.85 - as per USBR Water Measurement Manual), they are less sensitive to submergence effects. Hence it is required to study the effect of submergence with respect to sharp crested weirs which are relatively more sensitive to submergence.

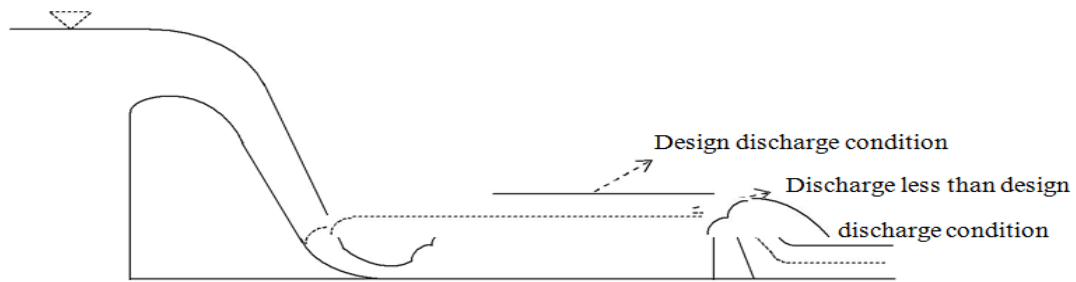


Fig. 3.3 Position of hydraulic jump at design and lower discharge for the end weir designed for design discharge condition

3.2 Governing Factors

The factors which govern design of stepped weir geometry are as follows –

Head on upstream	=	H
Width of channel	=	B
Maximum discharge in the range	=	Q_{\max}
Minimum discharge in the range	=	Q_{\min}
Coefficient of discharge	=	C_d
Submerged flow coefficient	=	K
Starting height of weir crest	=	y'

3.3 Development of mathematical procedure

The proposed stepped weir should cater to wide range of discharge from design discharge (Q_{\max}) to minimum discharge equal to 20% of the design discharge (Q_{\min}). 'N' intermediate discharges between Q_{\min} and Q_{\max} with an interval of $(Q_{\max} - Q_{\min}) / (N+1)$ are considered resulting in (N+2) discharges corresponding to which there would be (N+2) steps in a stepped weir. A stepped weir is considered to be made up of number of rectangular weirs. The equation for discharge Q over a rectangular sharp crested weir (free flow) is given by following equation

$$Q = \frac{2}{3} C_d b \sqrt{2g} (y_2 - y')^{\frac{3}{2}} \quad (1)$$

As $h = y_2 - y'$, the required width of weir can be expressed as (refer Fig.3.4)

$$b = \frac{3}{2} \frac{Q}{C_d \sqrt{2g} (y_2 - y')^{\frac{3}{2}}} \quad (2)$$

y_2 is calculated from Belanger momentum equation (Subramanya, 1986). As illustrated in Fig. 3.2, width of first step is given by

$$b_1 = \frac{3}{2} \frac{Q_1}{C_d \sqrt{2g} ((y_2)_1 - y')^{\frac{3}{2}}} \quad (3)$$

Where, $y' = (y_2)_1 / 4$ is designed for Q_1 (i.e. Q_{\min}). $(y_2)_1$ is the post jump depth corresponding to Q_1 and is calculated by Belanger momentum equation in the following manner.

$$(y_2)_i = \frac{(y_2)_i}{2} \left(-1 + \sqrt{1 + 8(Fr_1)^2} \right) \dots \dots \dots i \geq 1 \quad (4)$$

Where $(y_2)_i = \frac{Q_i}{BV}$, $V = \sqrt{2gH}$, $(Fr_1)_i = \frac{V_1}{\sqrt{gy_1}}$

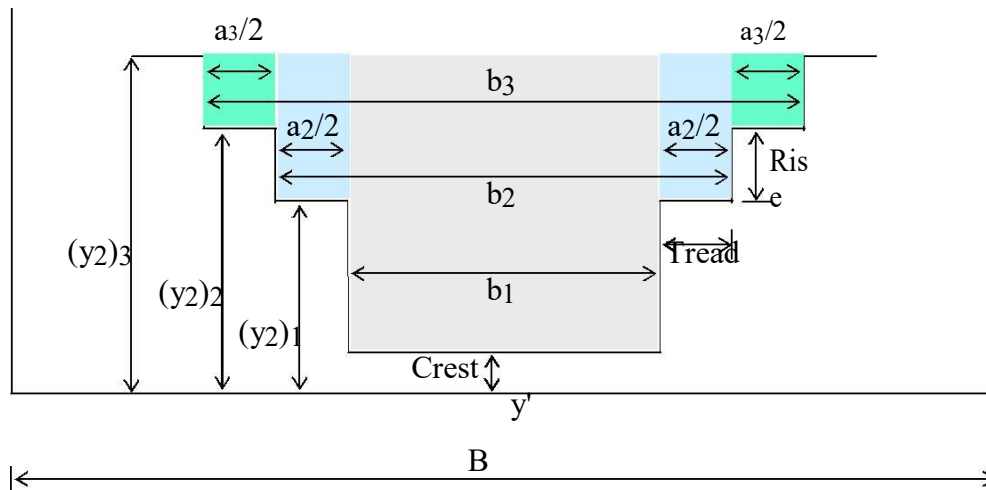


Fig. 3.4 Design of rectangular stepped weir (Section A-A taken from Fig. 3.1) (first 3-steps shown)

Using equation (2), for any discharge Q_n , the width of the corresponding step b_n can be calculated as follows,

$$b_n = b_{n-1} + a_n \dots \dots \dots n > 1 \quad (5)$$

Where a_n represents the incremental width at n^{th} step.

$$a_n = \frac{3}{2} \frac{Q_n - [\sum_{i=1}^{i=n-1} (Q_n)_i]}{C_d \sqrt{2g} ((y_2)_n - (y_2))^{\frac{3}{2}}} \quad (6)$$

$$\text{And } (Q_n)_i = \frac{2}{3} C_d b \sqrt{2g} ((y_2)_n - y')^{\frac{3}{2}} \quad (7)$$

The mathematical procedure is based on the free flow rectangular weir formulae. Here it is presumed that stepped weir is made up of number of rectangular weirs. As guidelines for stepped weir's C_d are not available, it is necessary to evolve C_d for free flow stepped weir. In practice, mostly the crest of stepped weir is submerged, therefore it becomes essential to evolve modified discharge coefficient which would be applicable to submerged conditions. More light is thrown on these aspects in the subsequent section.

In practice, mostly the crest of stepped weir is submerged, therefore it becomes essential to evolve modified discharge coefficient which would be applicable to submerged conditions. More light is thrown on these aspects in the subsequent sections.

Another aspect regarding mathematical procedure is about assumptions 2 and 5. In this design, supercritical velocity v_1 is calculated by the method suggested by Peterka (1984). C_d is calculated using formula given by Subramanya (1986). But it has generated a zig-zag geometry of stepped weir as shown in Fig. 3.5. Though mathematically correct, it is not practicable.

For each discharge, for calculation of y_2 , it is necessary to calculate corresponding prejump depth y_1 and thus corresponding prejump velocity v_1 . v_1 can be calculated by the procedure given by Peterka in USBR Monograph 25 (www.usbr.gov), that considers variation of head which is proportional to discharge. On the contrary, the assumption of 'H' to be constant, which in turn implies pre jump velocity also to be constant, gives a practical solution. As, finally the design of stepped weir is based on the magnitudes of post jump depths (y_2) for (N+2) discharges, these depths are calculated by both the methods discussed above. For this purpose data of an existing dam is considered.

$$B = 55\text{m}, H = 21.2\text{m}, Q_{\max} = 1736 \text{ m}^3/\text{s}, Q_{\min} = 347.2 \text{ m}^3/\text{s}.$$

It is found that the values of y_2 fairly agree with each other as correlation coefficient is found to be 0.99. The comparison of y_2 values is presented herewith for ready reference.

Table 3.1 Calculation of y_2 by two methods

Step No.	y_2 m - based on monograph method	y_2 m - based on proposed method
1	4.699	4.972
2	5.681	5.851
3	6.465	6.603
4	7.133	7.286
5	7.792	7.871
6	8.356	8.424
7	8.885	8.938
8	9.382	9.419
9	9.854	9.873
10	10.367	10.302
11	10.866	10.712

Fig. 3.4 shows a pattern of stepped weir which is mathematically correct as well as practicable. As an additional exercise, C_d values are calculated by the formula proposed by Swamee (1988). But it has also resulted into a similar zig-zag geometry of stepped weir. After extensive trials on mathematical model with different input data, it is found that even minute variation of H and C_d is resulting into an impracticable geometry of stepped weir.

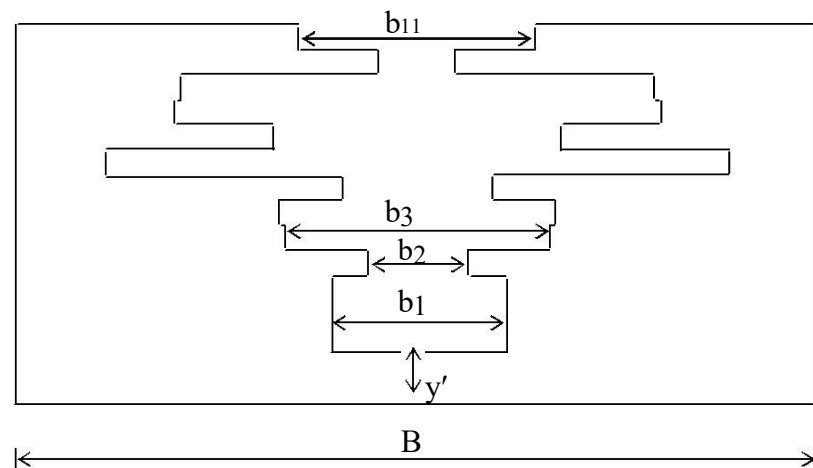


Fig. 3.5 Schematic of zig-zag geometry of stepped weir

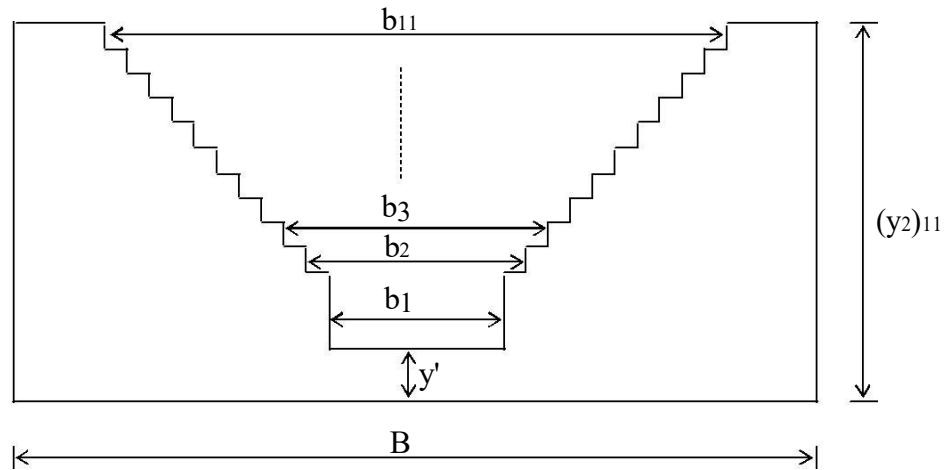


Fig. 3.6 Definition sketch of geometry of rectangular stepped weir

No literature is available on rectangular sharp crested stepped weir. Recently some work on compound broad crested weirs is reported by Jan et al (2006) and by Gogus et al (2009). Jan has investigated the rectangular-rectangular compound broad crested weir and derived the discharge equations for $0.2 \leq h/b_w \leq 0.34$. Gogus has investigated different compound broad crested weir geometries for $0.1 \leq h/b_w \leq 0.7$. Gogus further concluded that, for $h/b_w \geq 0.5$, the C_d values are almost remaining constant. In the case study discussed in chapter 6, the h/b_w ratio for the middle weir of step width b_1 (which is contributing more than 80% of the discharge for any y_2 on its upstream) ranges from 0.5 to 1.27. Thus, with the reasonable approximation, it is assumed to treat both H and C_d as constant throughout the design. It is found that for $Fr_1 > 4.5$, the mathematical procedure gives practicable geometry of stepped weir which is also mathematically correct.

3.4 Determination of Appropriate C_d for Free Flow Condition on Horizontal Apron

In the mathematical design of stepped weir, for free flow condition, a constant value of $C_d = 0.623$ is adopted according to Francis formula. As there are different kinds of uncertainties involved in the flow conditions, the analytical determination of C_d is hardly possible. To mention a few, there is presence

hydraulic jump and associated turbulence on upstream of stepped weir. The upstream reach for the stepped weir, being equal to length of stilling basin, is small. Hence it is decided to empirically judge the appropriateness of C_d by the appropriateness of hydraulic jump position (which is vulnerable to uncertainties due to some assumptions involved in the mathematical design of weir) which is the main aim of study. Being an implicit function, C_d needs to be assumed at initial stage. If the weir performance is not satisfactory the step widths can be modified empirically. It is proposed to conduct tests in ANSYS software under free flow condition. For creating free flow conditions over the stepped weir, the bottom of channel in the first half (2m long) is raised.

Common parameters for which weirs are designed are $H=0.4\text{m}$, $B=0.3\text{m}$, $Q_{\max}=0.01\text{ m}^3/\text{s}$, $Q_{\min}=0.002\text{ m}^3/\text{s}$, $y'=0.015\text{m}$. Three weir models, each for $C_d=0.6$, 0.65 and 0.623 are designed. As per present practice, energy dissipators are designed for the design discharge conditions and their performance is tested at lower discharges (Vittal and Al-Garni 1992). Generally apart from design discharge, the performance is tested at 3 lower discharges which are 75%, 50% and 25% of design discharge. To increase the accuracy, it is proposed to consider 10 lower discharges and reduce the lowest discharge to 20% of design discharge. Thus, including design discharge, there would be total 11 discharges. Thus in the proposed stepped weir, there are 11 steps corresponding to 11 discharges. Tables 3.2 (a, b and c) give the geometry of these weirs and other parameters related to hydraulic jump.

Table 3.2 (a) Output of Mathematical Procedure Data
(Horizontal apron and $C_d=0.6$)

Sr.No.	Q m ³ /s	y1 m	y2 M	h m	Fr1	B M
1	0.0020	0.0024	0.0605	0.0455	18.3350	0.1162
2	0.0028	0.0033	0.0714	0.0564	15.4960	0.1387
3	0.0036	0.0043	0.0807	0.0657	13.6661	0.1519
4	0.0044	0.0052	0.0889	0.0739	12.3614	0.1629
5	0.0052	0.0062	0.0965	0.0814	11.3709	0.1723
6	0.0060	0.0071	0.1034	0.0884	10.5857	0.1808
7	0.0068	0.0081	0.1098	0.0948	9.9435	0.1885
8	0.0076	0.0090	0.1159	0.1009	9.4056	0.1957
9	0.0084	0.0100	0.1216	0.1066	8.9466	0.2024
10	0.0092	0.010947	0.1270	0.1120	8.5487	0.2087
11	0.0100	0.011899	0.1322	0.1172	8.1997	0.2147

With $C_d = 0.6$, the performance of weir is tested for boundary conditions of discharge, that are Q_{min} and Q_{max} to check the possibility of jump formation and the adequacy of its location. It is presumed that if the weir performance is unsatisfactory over these extreme discharges, then it would probably be unsatisfactory for the intermediate discharges also. The jumps are found to be shifted in the downstream direction for both the discharges. This shows that the area of flow section of stepped weir is larger and need to be reduced. This can be done by reducing the step widths(b) which requires increase of C_d as b varies inversely with C_d .

Table 3.2 (b) Output of Mathematical Procedure for Data
(Horizontal apron and $C_d = 0.65$)

Sr.No.	Q m ³ /s	y1 m	y2 m	h m	Fr1	B M
1	0.0020	0.0024	0.0605	0.0455	18.3350	0.1073
2	0.0028	0.0033	0.0714	0.0564	15.4960	0.1280
3	0.0036	0.0043	0.0807	0.0657	13.6661	0.1403
4	0.0044	0.0052	0.0889	0.0739	12.3614	0.1504
5	0.0052	0.0062	0.0965	0.0814	11.3709	0.1591
6	0.0060	0.0071	0.1034	0.0884	10.5857	0.1669
7	0.0068	0.0081	0.1098	0.0948	9.9435	0.1740
8	0.0076	0.0090	0.1159	0.1009	9.4056	0.1806
9	0.0084	0.0100	0.1216	0.1066	8.9466	0.1868
10	0.0092	0.010947	0.1270	0.1120	8.5487	0.1926
11	0.0100	0.011899	0.1322	0.1172	8.1997	0.1981

In the second trial another stepped weir is designed with $C_d = 0.65$ and tested in a similar manner. During this, the jumps are found to be drowned. Hence for the third trial $C_d = 0.623$ is adopted and accordingly, tests are taken.

For stepped weir with $C_d = 0.623$, the hydraulic jumps have formed inside the basin and the fronts of jumps in all the cases were found to be located near the sluice gate. Thus $C_d = 0.623$ is confirmed empirically for the condition of free flow over the weir. For higher submergences ($S_r > 0$), the coefficient of discharge will decrease and takes the form of modified coefficient of discharge ($C_{dm} = k_s C_d$, where $k_s < 1$). In this case, k_s is a submerged flow coefficient for stepped weir which is newly introduced. Determination of C_{dm} based on K_s is explained below.

Table 3.2 (c) Output of Mathematical Procedure for Data
(Horizontal apron and $C_d = 0.623$)

Sr.No.	Q m ³ /s	y ₁ M	y ₂ m	H M	F _{r1}	B M
1	0.0020	0.0024	0.0605	0.0455	18.3350	0.1119
2	0.0028	0.0033	0.0714	0.0564	15.4960	0.1336
3	0.0036	0.0043	0.0807	0.0657	13.6661	0.1463
4	0.0044	0.0052	0.0889	0.0739	12.3614	0.1569
5	0.0052	0.0062	0.0965	0.0814	11.3709	0.1660
6	0.0060	0.0071	0.1034	0.0884	10.5857	0.1741
7	0.0068	0.0081	0.1098	0.0948	9.9435	0.1816
8	0.0076	0.0090	0.1159	0.1009	9.4056	0.1884
9	0.0084	0.0100	0.1216	0.1066	8.9466	0.1949
10	0.0092	0.010947	0.1270	0.1120	8.5487	0.2010
11	0.0100	0.011899	0.1322	0.1172	8.1997	0.2067

3.5 Determination of Appropriate C_{dm} for Submerged Flow Condition on Horizontal Apron

When tail water depth (y_t) rises above crest, weir is said to be submerged. For determination of C_{dm} , it is necessary to determine k_s . The effect of tail water submergence is discussed in USBR publications like Monograph 25 (1984), Manual of Water Measurement (2001) and Design of Small Dams (1974). In 1947 Villemonte (Subramanya 1986) has studied effect of submergence on discharge over rectangular sharp crested suppressed weir and has given a relation between k and S_r . But a similar detailed analysis is not available for rectangular stepped weir. Thus for stepped weir, k_s (for given S_r) is determined empirically and is compared with k – for rectangular weir given by following Villemonte's equation.

$$K = \frac{Q_s}{Q_f} \tag{8}$$

Where, Q_s and Q_f are the submerged and free flow discharges respectively and S_r

$$S_r = \frac{y_t - y'}{y_2 - y'} \quad (9)$$

To find k_s empirically, 6 stepped weir sections with different k_s values ranging from 1 to 0.8 at an interval of 0.04 are designed. The other design parameters are same as before. The weir sections performance are tested in ansys for corresponding ranges of S_r . Submergence is created by putting step wise blockage at the end of the channel instead of operating tail gate. Use of vertical stop logs ensures continuation of stream lines. The performance of weir section is judged from the ability of weir section to form clear hydraulic jumps at appropriate position for boundary discharges. The details of the trials are given below.

In order to obtain ' k_s ', series of performance in ansys fluent are carried out . The experimentation is carried out for three mean submergence ratios viz. 0.45, 0.65 and 0.75 and accordingly three k_s values are determined. Once relation between S_r and k_s is established, a relation between S_r and C_{dm} can be obtained and it can be used for practical applications.

In the first trial appropriateness of C_d for free flow condition of stepped weir is determined empirically. In the second trial, the raised platform is removed from the flume and tail water depths are raised to create submergence conditions on downstream of stepped weir. The submergence so created is kept proportional to discharge. Over a range of discharge and a corresponding range of S_r (0.4 to 0.5), again a stepped weir with $C_d=0.623$ (i.e. $k=1$) is tested. It is observed that for both the discharges drowned jumps are formed. This indicates that the area of flow at the stepped weir section is not adequate to form clear jumps near sluice gate. Then next weir section with $C_{dm} = 0.6$ (i.e. $k_s=0.96$ and having relatively large area of flow than the previous case) is tested and it has formed clear jumps at appropriate location. This has confirmed that stepped weir under consideration is operating satisfactorily. Further to reconfirm the adequacy of this stepped weir, for the same submergence conditions a weir section with $C_{dm} = 0.57$ (i.e. $k_s=0.92$) is tested and it is observed that the front of jump moved away from

the appropriate position(i.e. swept up jump). Thus the value of $C_{dm} = 0.6$ for the average $S_r = 0.45$ is finally confirmed. Similar tests are carried out with average submergence ratios 0.65 and 0.75 and the corresponding values of C_{dm} are found to be 0.55 and 0.5 (i.e. $k_s = 0.88$ and 0.8) respectively. Table 3.2 gives comparison of empirically determined k_s values with k value given by villemonte.

Table 3.3 Comparison of submerged flow coefficients k and k_s

Sr. No.	Range of Submergence ratio (S_r)	Average Submergence ratio (S_r)	k	k_s	$C_{dm} = k_s \times C_d$
1	0.4 to 0.5	0.45	0.87	0.96	0.6
2	0.6 to 0.7	0.65	0.75	0.88	0.55
3	0.7 to 0.8	0.75	0.67	0.80	0.5

The values of K_s are slightly greater than k . This is because of following approximations involved in the process.

- iv) Villemonte's equation (which is applicable to rectangular weir) is applied to stepped weir.
- v) In conventional rectangular weirs the whole crest of weir is under submergence. But in case of stepped weir, crest and few steps are under submergence.
- vi) In conventional weirs the flow on upstream is gentle. Whereas in present case there is presence of hydraulic jump on upstream of stepped weir.

3.6 Closure

A new stilling basin design is proposed in the form of horizontal apron with a stepped weir at its end. A mathematical procedure is developed to design geometry of rectangular sharp crested stepped weir for various operating conditions. In case of horizontal apron, a new parameter - submerged flow coefficients (k_s) is introduced and is determined empirically for different average submergence ratios (S_r). A relationship between S_r and C_{dm} is established for horizontal apron. The equation for close starting height of weir (y') is given. To optimize geometry of stepped weir, few trials with mathematical procedure are required to be taken with values around y' .

Chapter 4

CFD Studies and Results

4.1 Computational Fluid Dynamics

CFD has certainly come of age in industrial applications and academic research (Tu et al 2008). In the beginning CFD was mainly limited to area of aeronautics, but now it is widely adopted methodology for solving complex problems in many engineering fields. CFD can be employed to better understand the physical events or processes that occur in the flow of fluids around and within the designated objects. These events are closely related to the action and interaction of phenomena associated with dissipation, diffusion, convection, boundary layer and turbulence. Thus it can be employed as a research tool to perform numerical experiments. There are various commercial CFD packages available like Fluent, Flow 3-D and Star CD. In the current study Fluent is used. Performance of weir is tested on Fluent.

4.2 Numerical modeling

The numerical modeling involves the solution of Navier-Stokes equations, which are based on the assumptions of conservation of mass and momentum within a moving fluid. The conservation of mass is described by the differential equation

$$\frac{\partial \rho}{\partial t} + \nabla (\rho v) = 0 \quad (1)$$

Where ρ is the density and v is the velocity of the fluid. The conservation of momentum is similarly described as

$$\frac{\partial (\rho v)}{\partial t} + \nabla (\rho v v) = -\nabla p + \nabla \tau \quad (2)$$

Where p is the pressure and τ is the stress tensor. In order to represent the effects of turbulence on the flow, additional transport equations are solved for various turbulence quantities. To represent the sharp interface between the air and water, the Volume of Fluid (VOF) method is used. In this method, the interface is tracked by introducing the volume fraction α_i , where i refers to the phase. The volume fraction for the i^{th} phase is the fraction of the volume of a cell occupied by that volume. When modeling the free surface between water and air, a transport equation is solved for the water phase.

$$\frac{\partial \alpha_w}{\partial t} + \nabla \cdot (\mathbf{v} \alpha_w) = 0 \quad (3)$$

Where, α_w is volume fraction of water. The volume fraction for the other phase (say air) is,

$$\alpha_a = 1 - \alpha_w \quad (4)$$

Where, α_a is volume fraction of air. The finite volume method is used to solve the above equations and relies on the flow domain being divided into a grid consisting of a large number of cells. In each cell, if it contains only water, then $\alpha_w = 1$; if none, then $\alpha_w = 0$. For cells that span the interface between the air and water, $0 < \alpha_w < 1$. The fluid properties in each cell are adjusted according to the local volume fraction, for example, the density in each cell is,

$$\rho = \alpha_w \rho_w + (1 - \alpha_w) \rho_a \quad (5)$$

Similar expression can be used for dynamic viscosity μ .

4.3 CFD Model Setup

For hydraulic jump simulation in rectangular channel, commercially available general purpose CFD solver - Fluent 6.3.26 has been used (Fluent Inc 2006). Geometry of experimental setup and meshing are done in Gambit 2.3.16 (Fluent Inc 2006). The VOF model is used for multiphase fluid (i.e. two phase mixture of water and air) to capture interface between water and air (Hargreaves et al 2007).

Fluent solves Reynolds Averaged Navier-Stokes (RANS) equations. These are transport equations for momentum, which simplify the flow physics by averaging out turbulent fluctuations in velocity and pressure, but thereby incur penalty of extra unknown correlations, the Reynolds stresses (Hargreaves et al 2007). The latter are approximated in a process known as turbulence modeling and the results reported here are obtained using the SST $k-\omega$ model. $k-\omega$ is a turbulence model developed by Wilcox in 1998 (Tu et al 2008). Here ω is a frequency of large eddies which are formed close to walls in boundary layer flows. $k-\omega$ model is very sensitive to the free stream value of ω but it works exceptionally well under adverse pressure gradients. Standard $k-\epsilon$ model is less sensitive to free stream values but is often inadequate under adverse pressure gradients. Thus in 1998 Menter proposed to combine both standard $k-\epsilon$ and $k-\omega$ model, which

retains the properties of $k-\omega$ close to the wall and gradually blends into standard $k-\epsilon$ model away from the wall. This combined model is known as Shear Stress Transport (SST) $k-\omega$ model. This model is very useful in capturing hydraulic jump and the velocity vectors in it.

In the VOF method used here, a single set of transport equations for momentum, turbulence kinetic energy k and its dissipation rate ω is solved for the air and water phases, together with a transport equation for the volume fraction of the water phase. The latter is 1 or 0 for water and air filled cells respectively; for cells spanning the free surface it takes an intermediate value. The properties in the transport equations, density ρ and dynamic viscosity μ , are the volume fraction averaged values (Sarkar and Rhodes 2004).

4.4 Preprocessing

Preparation of Geometry and meshing in Gambit

To evaluate performance it is proposed to set up stepped weir in Fluent model. Fig. 4.1 shows the experimental setup and Fig. 4.2 shows 3-dimensional geometry of experimental setup prepared in Gambit.

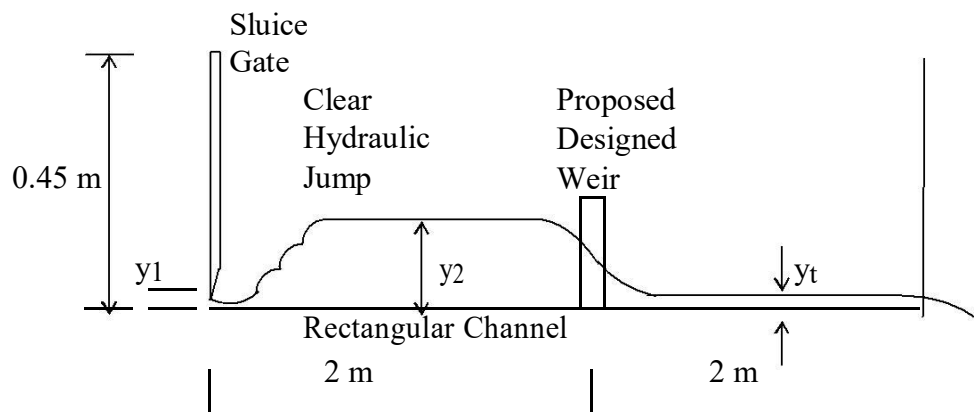


Fig. 4.1 Experimental Setup

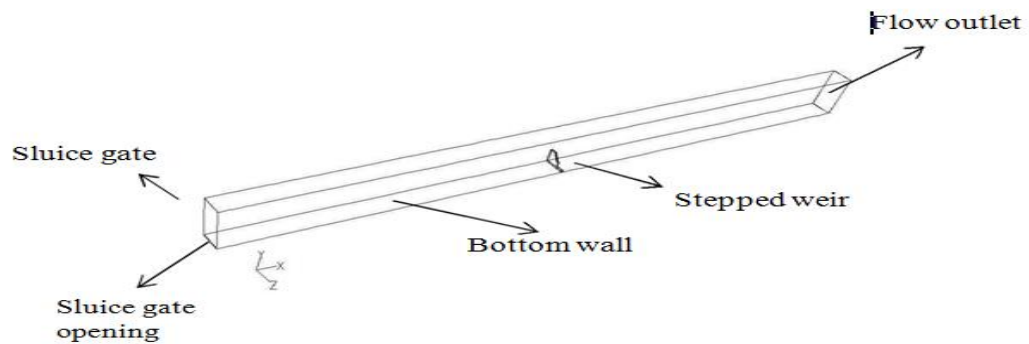


Fig 4.2 Schematic of problem setup prepared in gambit

The details of various components are given below.

- 1) A 3-dimensional rectangular channel of exactly same dimensions as that of laboratory tilting flume (general size) is prepared in gambit.
- 2) A structured hexahedral mesh is used for meshing as it grants accurate results (Gambit user's guide 2006). A dense mesh is prepared in the zones where the boundary layer effects are predominant, that is near bed and junctions of bed and sides (Christopher and Marshall 2001). To reduce the cell count in order to speed up convergence (Chippada et al 1994), the domain is made half by cutting it longitudinally as it is symmetrical. A 400 x 20 x 15 (x x y x z) non-uniform, rectangular grid having 4,87,150 hexahedral cells is used.
- 3) The mesh is transported to Fluent.

The mesh is imported in Fluent. The initial parameters which are set in Fluent are 3ddp, pbns, vof, sstk ω and unsteady. These parameters are briefly explained below.

3ddp	-	3 dimensional double precision.
Pbns	-	pressure based navier stoke
Vof	-	volume of fluid
Sstk ω	-	shear stress transport k ω
Unsteady	-	Solution initiated with unsteady flow condition

The use of k- ω formulation in the inner parts of the boundary layer makes the model

directly usable all the way down to the wall through the viscous sub-layer. The SST formulation also switches to a $k-\varepsilon$ behavior in the free-stream and thereby avoids the common $k-\omega$ problem that the model being too sensitive to the inlet free – stream turbulence properties. It is this feature that gives SST $k-\omega$ model an advantage in terms of performance over both the standard $k-\omega$ model and the standard $k-\varepsilon$ model.

4.4.1 Boundary Conditions

Velocity inlet boundary condition is applied at the sluice gate opening. At a distance of 4m downstream of inlet, the flow exits from a pressure outlet boundary. The weir is located at a distance of 2m downstream of inlet. All the walls (weir, side walls and bottom wall) are given a no slip shear boundary condition. The top face of channel is given the ‘symmetry’ boundary condition. For the bottom wall, roughness is taken into account. In Fluent, the roughness is expressed in terms of ‘wall roughness height’- K_s in meters and ‘wall roughness constant’- C_s . K_s is obtained from Manning’s roughness coefficient for mild steel bed and C_s is taken to be 0.5. The C_s value of 0.5 shows uniformity of roughness height. It reproduces Nikuradse’s resistance for pipe’s roughness with tightly packed uniform sand grains. When C_s is less than 0.5, it means the pipe is smooth and when it is greater than 0.5, it means pipe is rough. If no boundary condition is specified, by default fluent treat it as ‘wall’ boundary.

4.4.2 Descretization

To complete the description of the CFD modeling, the PRESTO pressure descretization scheme is used. First order descretization schemes are used for the momentum, turbulent kinetic energy and specific dissipation rate. This is because there is problem with second order upwind schemes as they exhibit the oscillatory behavior in the vicinity of discontinuities similar to that encounter with second order central difference schemes (Anderson 1995). The SIMPLE pressure velocity coupling algorithm is used.

For the volume fraction, automatic time step refinement in Fluent is used (Zhao et al 2004). A converged steady state solution is identified by low residuals in the finite volume equations and a near steady free surface profile.

As an initial condition for the solution, a volume fraction of 1 (corresponding to water) is patched for the region with length 0.20 m (from sluice gate), width 0.15m (half

symmetry) and height equal to sluice gate opening. Solution is then advanced in transient mode adopting a variable time stepping. The solution is run for 60 seconds. The results are summarized below.

Table 4.1 Comparison of post jump depths for horizontal apron – experimental and fluent (For $C_{dm} = 0.6$)

Test No.	Discharge $Q \text{ m}^3/\text{s}$ (Fluent)	Post jump Depth $y_2 \text{ m}$ (experimental)	Post jump depth $y_2 \text{ m}$ (Fluent)	Tail water depth $y_t \text{ m}$ (Fluent)	Submergence Ratio S_r (Fluent)
1	0.0100	0.124	0.1210	0.063	0.453
2	0.0088	0.120	0.1161	0.059	0.435
3	0.0075	0.110	0.1089	0.056	0.437
4	0.0067	0.107	0.1040	0.049	0.382
5	0.0052	0.092	0.0913	0.041	0.341
6	0.0048	0.087	0.0869	0.035	0.278
7	0.0024	0.063	0.0621	0.028	0.276

Table 4.2 Comparison of post jump depths for horizontal apron –

experimental and fluent (For $C_{dm} = 0.55$)

Test No.	Discharge $Q \text{ m}^3/\text{s}$ (Fluent)	Post jump Depth $y_2 \text{ m}$ (Experimental)	Post jump depth $y_2 \text{ m}$ (Fluent)	Tail water Depth $y_t \text{ m}$ (Fluent)	Submergence Ratio S_r (Fluent)
1	0.0100	0.123	0.1140	0.0540	0.394
2	0.0088	0.122	0.1110	0.0510	0.375
3	0.0075	0.112	0.1035	0.0475	0.367
4	0.0067	0.110	0.1010	0.0464	0.365
5	0.0052	0.091	0.0850	0.0363	0.304
6	0.0048	0.085	0.0810	0.0330	0.273
7	0.0024	0.062	0.0587	0.0270	0.275

Table 4.3 Comparison of post jump depths for horizontal apron – experimental and fluent (For $C_{dm} = 0.5$)

Test No.	Discharge $Q \text{ m}^3/\text{s}$ (Fluent)	Post jump Depth $y_2 \text{ m}$ (Experimental)	Post jump depth $y_2 \text{ m}$ (Fluent)	Tail water Depth $y_t \text{ m}$ (Fluent)	Submergence Ratio S_r (Fluent)
1	0.0100	0.126	0.1128	0.044	0.297
2	0.0088	0.120	0.1040	0.043	0.315
3	0.0075	0.112	0.1028	0.039	0.273
4	0.0067	0.109	0.0940	0.036	0.266
5	0.0052	0.093	0.0840	0.032	0.246
6	0.0048	0.085	0.0800	0.031	0.246
7	0.0024	0.062	0.0570	0.027	0.286

It is evident from Table 4.1 that fluent is capable to handle complex phenomenon like hydraulic jump. The results obtained are satisfactory. Later on additional tests are taken to gain more confidence for performance of fluent. During additional trials, two weir sections are tested for the corresponding tail water submergence conditions. Tables 4.2 and 4.3 show results of these trials. It is observed that the post jump depths as well as the tail water depths generated in Fluent are lesser than the corresponding experimental values. Therefore the submergence ratios obtained in Fluent are also on the lower side than the corresponding experimental values. But, surprisingly it is observed that in all the cases hydraulic jumps have formed near the sluice gate. As in case of $C_{dm} = 0.55$ and 0.5, the tail water submergence could not be reproduced and is lower than 0.4, as if we are dealing with free flow conditions. There should be jump sweep out condition in such cases. But in Fluent, both of these sections did not show any sweep out of hydraulic jump.

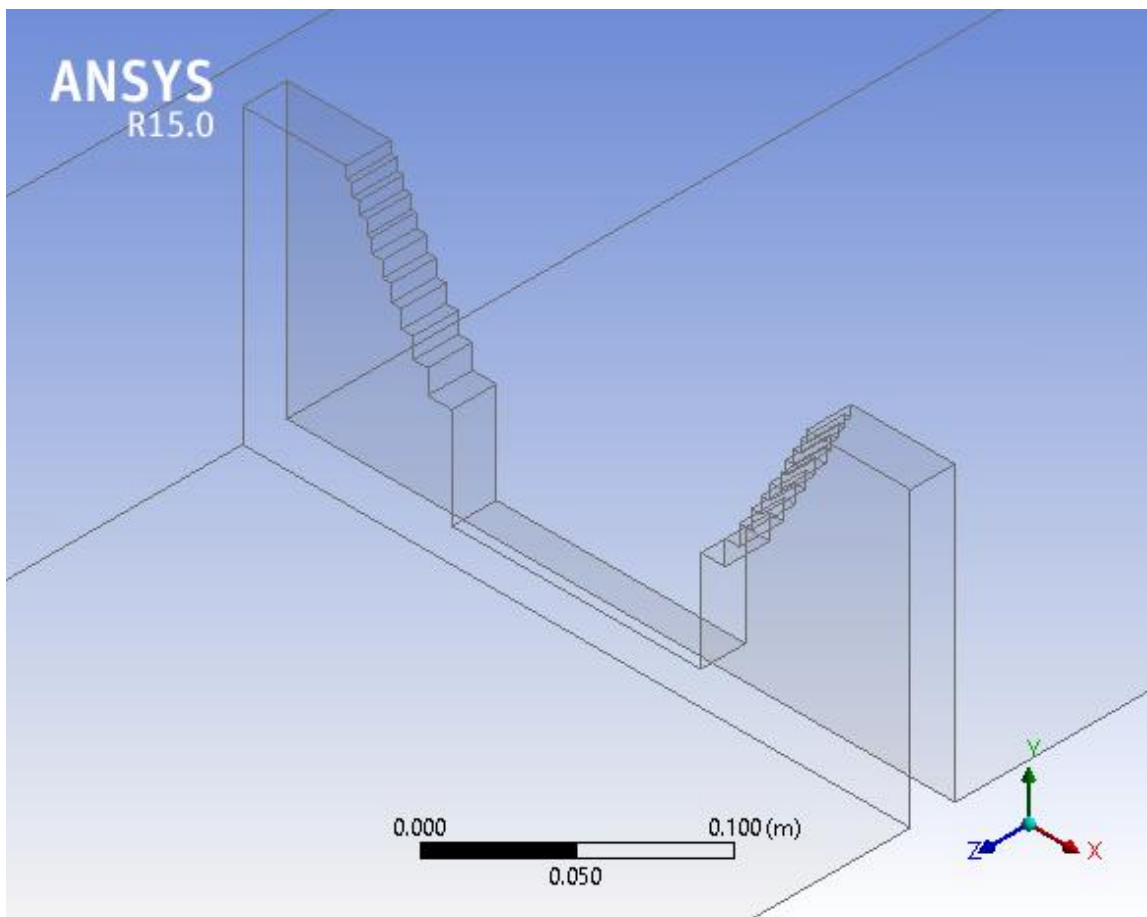


Fig 4.3 View of stepped weir section resting on channel bottom (obtained in Fluent)

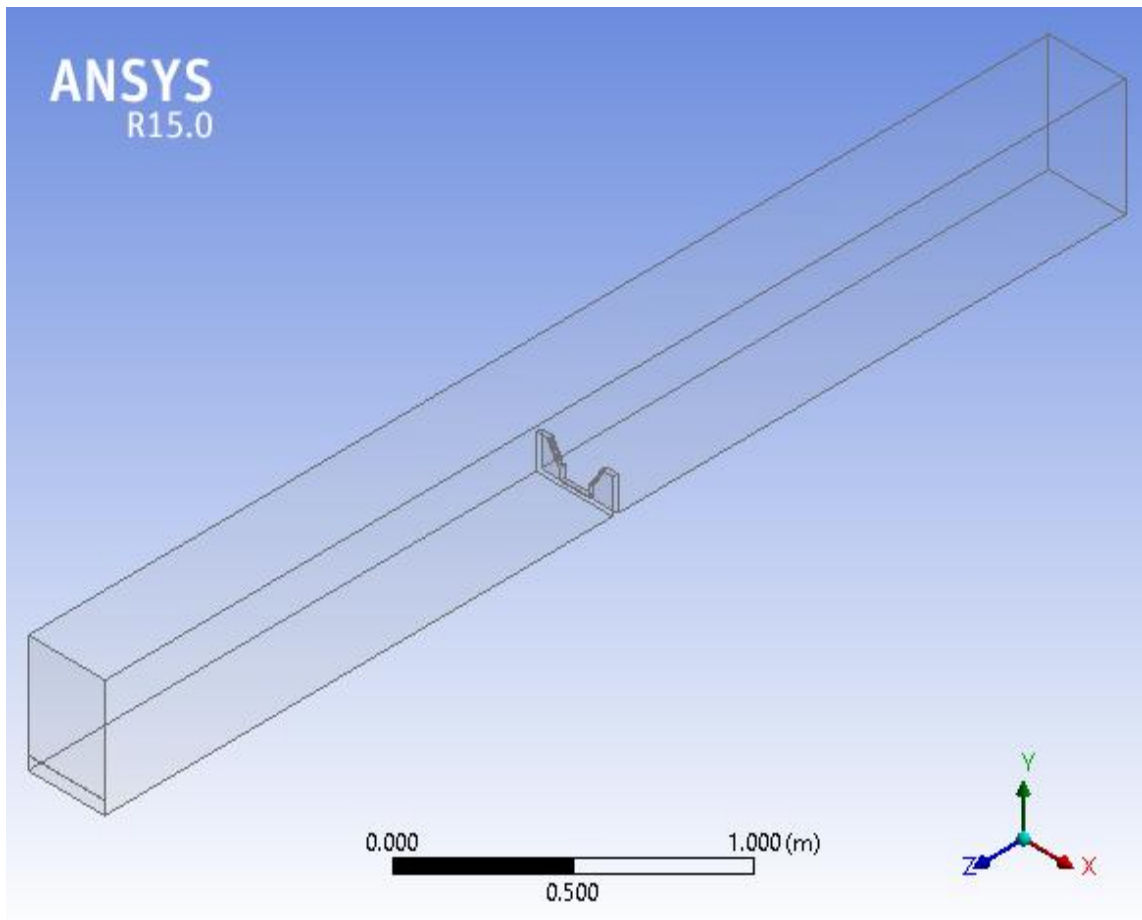


Fig 4.4 flume section with Stepped weir

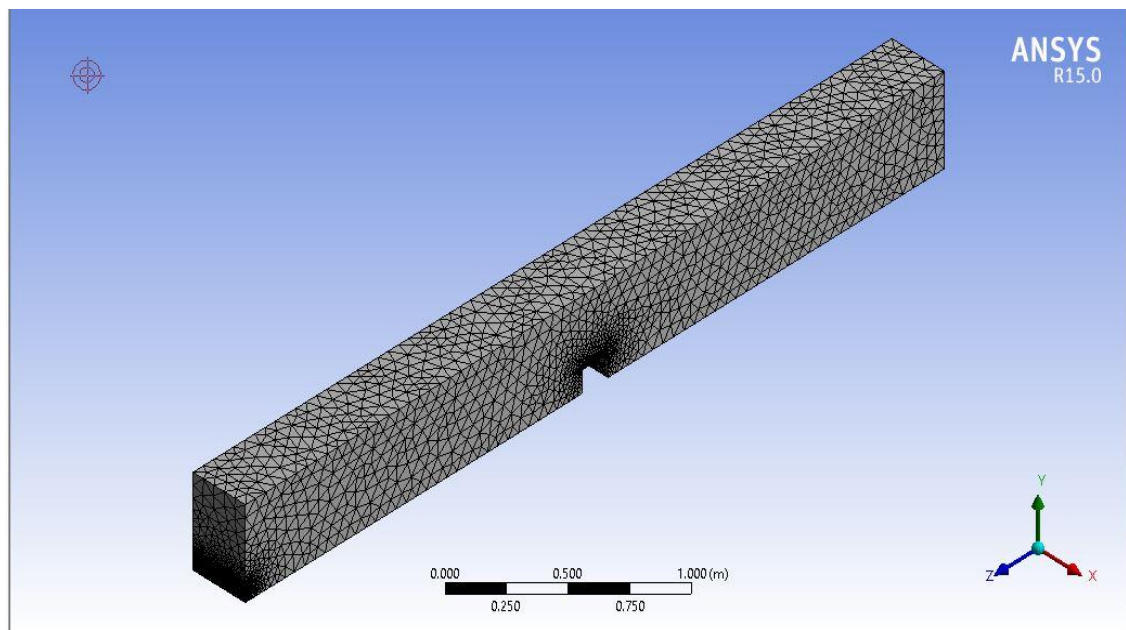


Fig 4.5 flume in meshed form

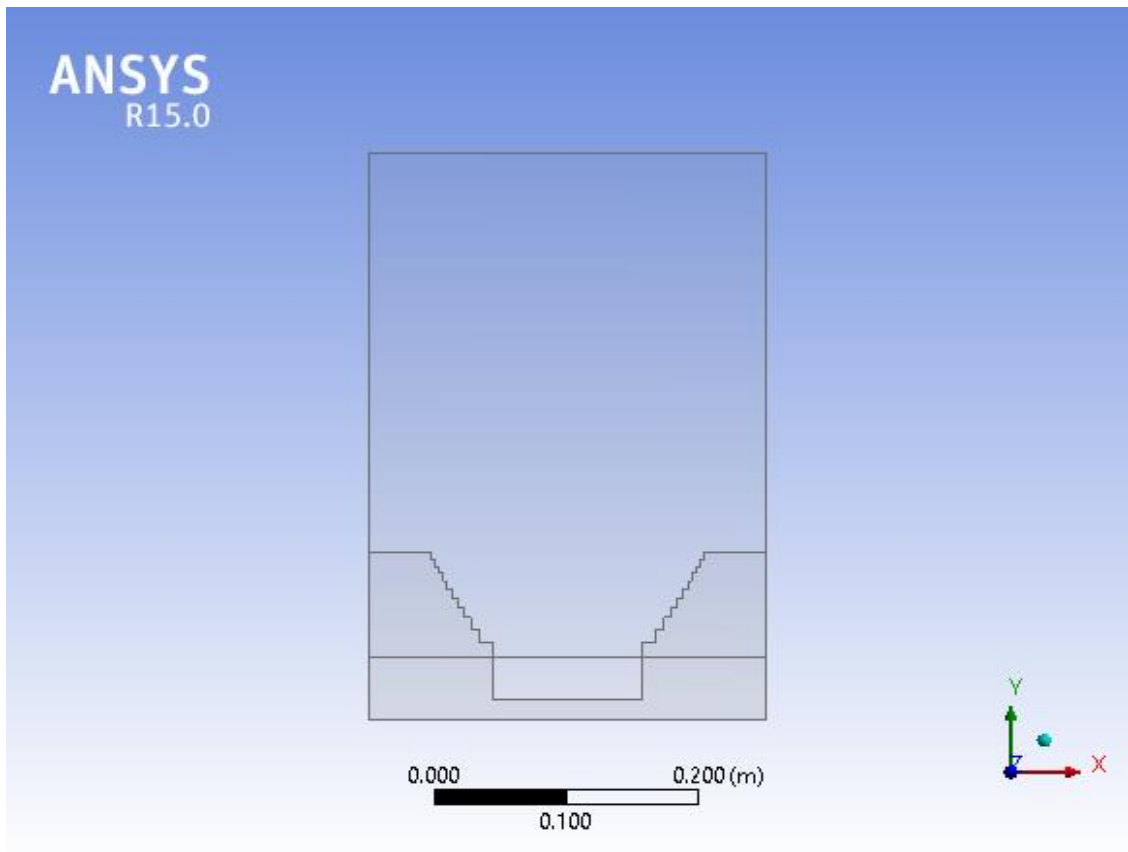


Fig 4.6 vertical view of stepped weir

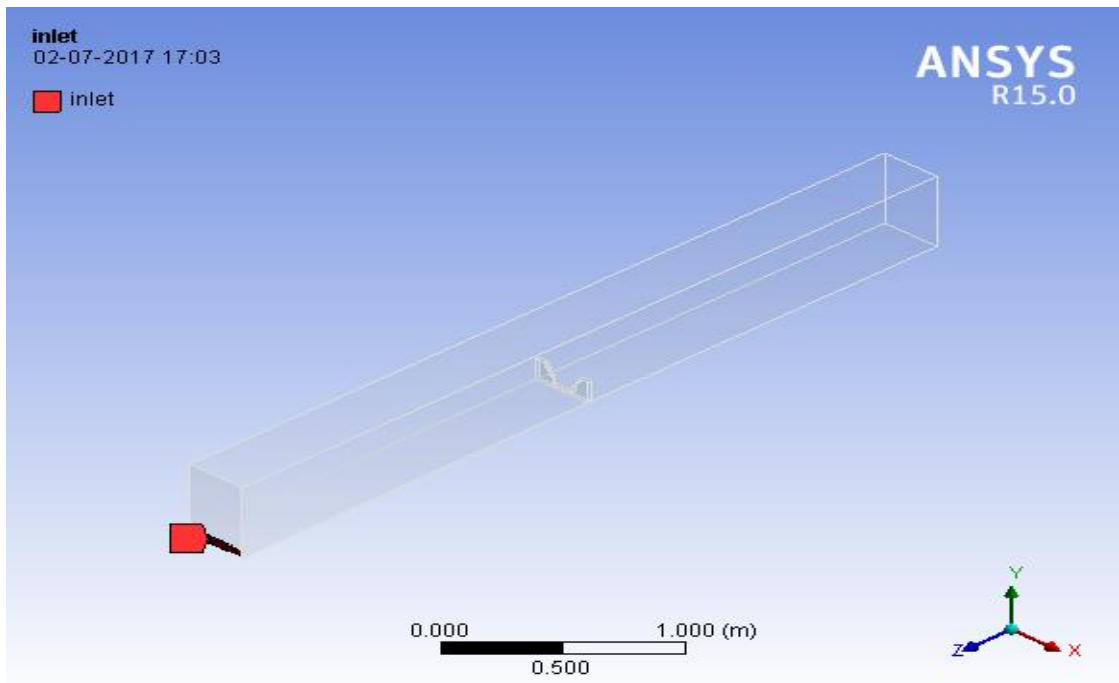


Fig 4.7 flow inlet section in flume

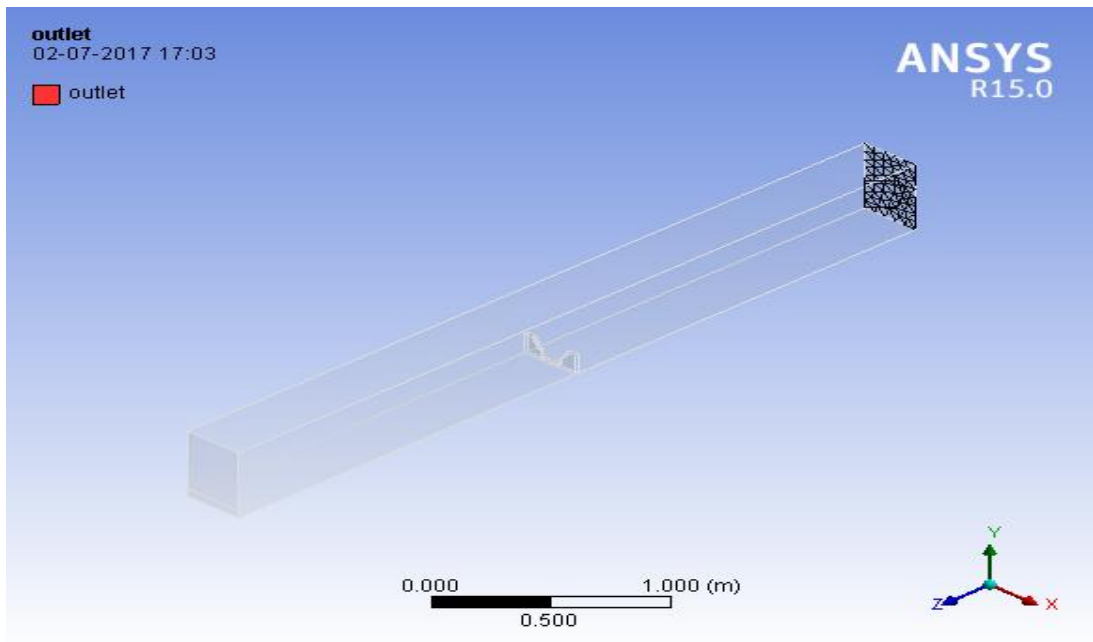


Fig 4.8 flow outlet in flume

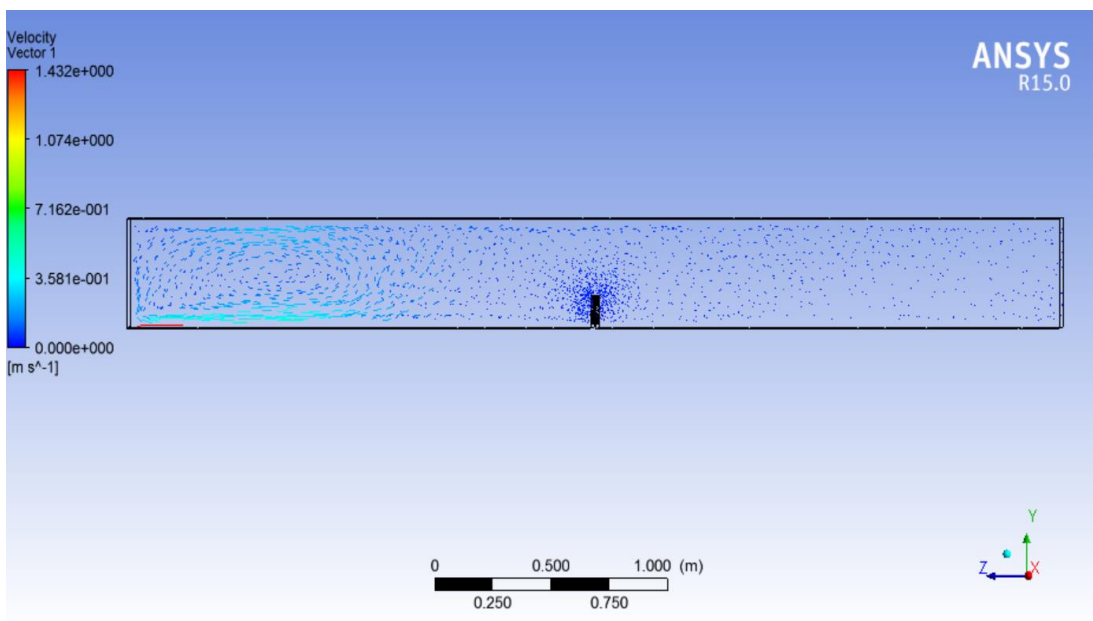


Fig 4.9 hydraulic jump at toe for discharge 0.0020 m³ /sec

At the lower discharge (20%) it was found that jump of small intensity are occurring on toe of spillway and length of jump was less and within the span of stilling basin. Hydraulic jump phenomenon became stable after 35 second in ansys fluent.

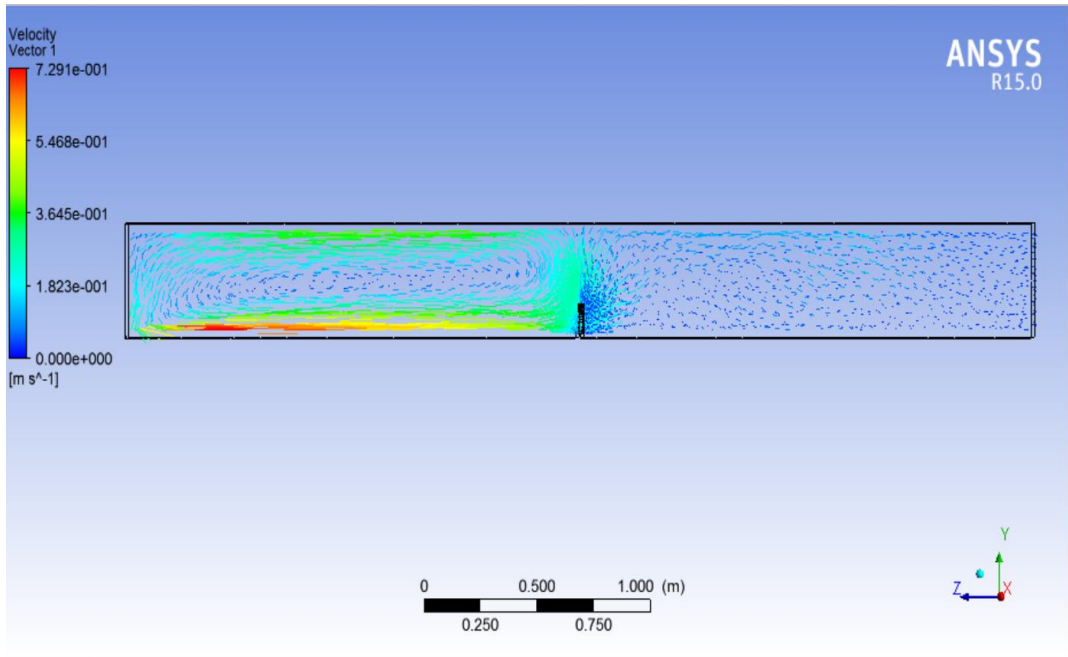


Fig 4.10 hydraulic jump at toe for discharge $0.0052 \text{ m}^3/\text{s}$

At the medium discharge (50%) it was found that jump of large intensity are occurring on toe of spillway and length of jump was more and restricted within the span of stilling basin with the help of stepped weir . Hydraulic jump phenomenon became stable after 40 second in ansys fluent.

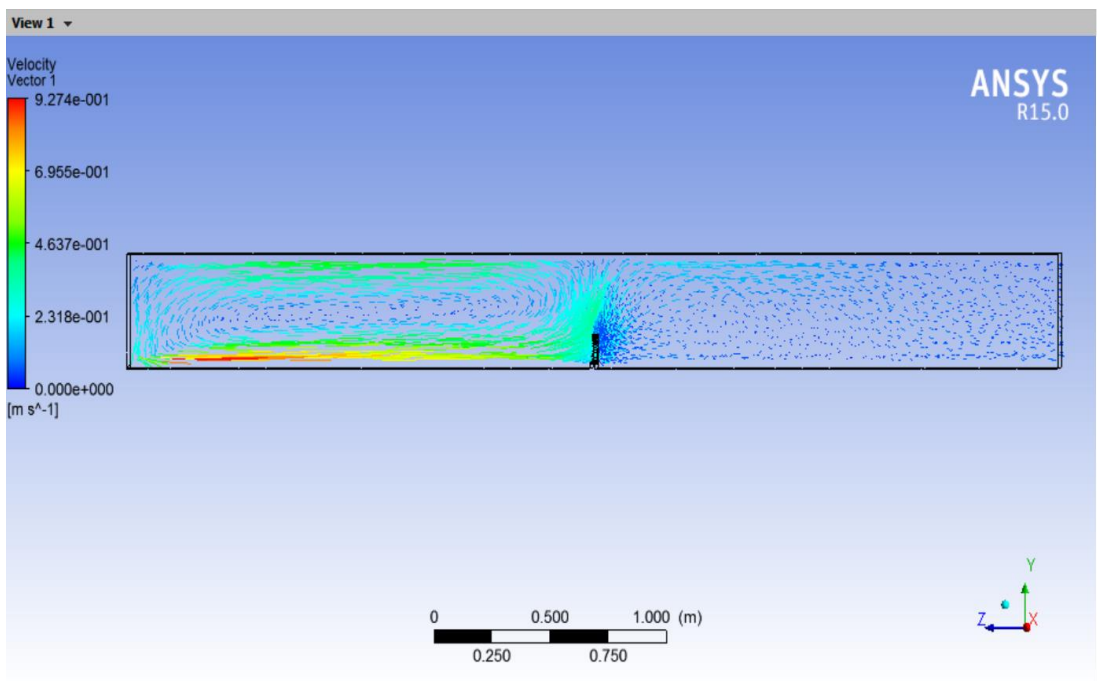


Fig 4.11 hydraulic jump at toe for discharge of $0.0068 \text{ m}^3/\text{s}$

At the discharge (68%) it was found that jump of sufficient intensity are occurring on toe of spillway and length of jump was more and restricted within the span of stilling basin with the help of stepped weir. Hydraulic jump phenomenon became stable after 40 second in ansys fluent.

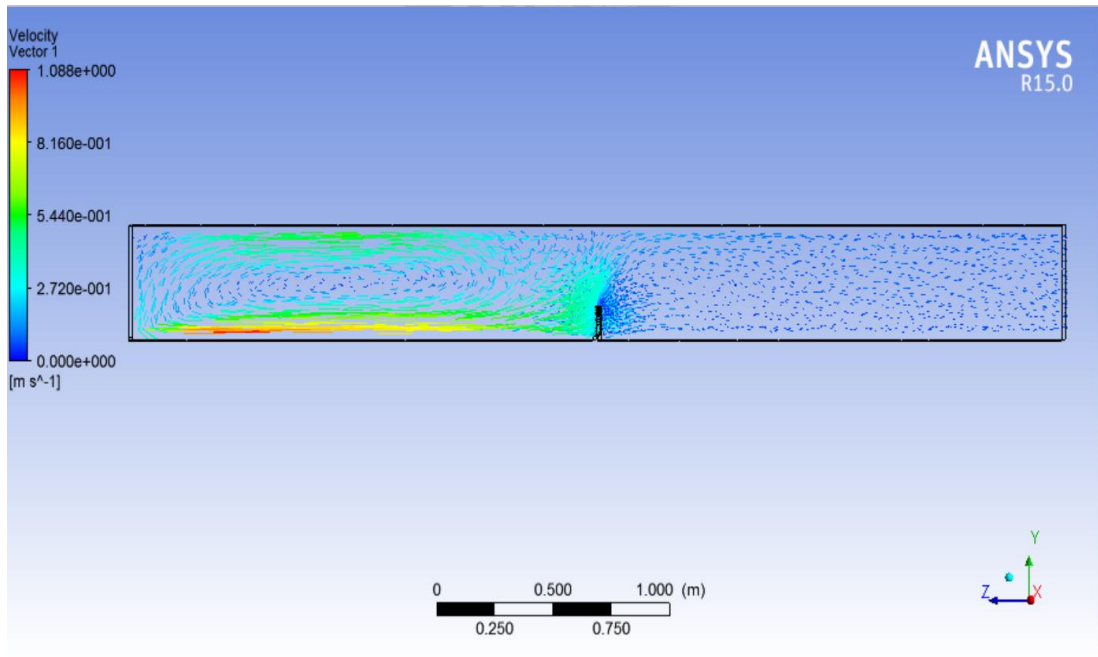


Fig 4.12 hydraulic jump at toe for discharge of 0.0084 m³/s

At the discharge (84%) it was found that jump of strong intensity are occurring on toe of spillway and length of jump was more and restricted within the span of stilling basin with the help of stepped weir . Hydraulic jump phenomenon became stable after 40 second in ansys fluent.

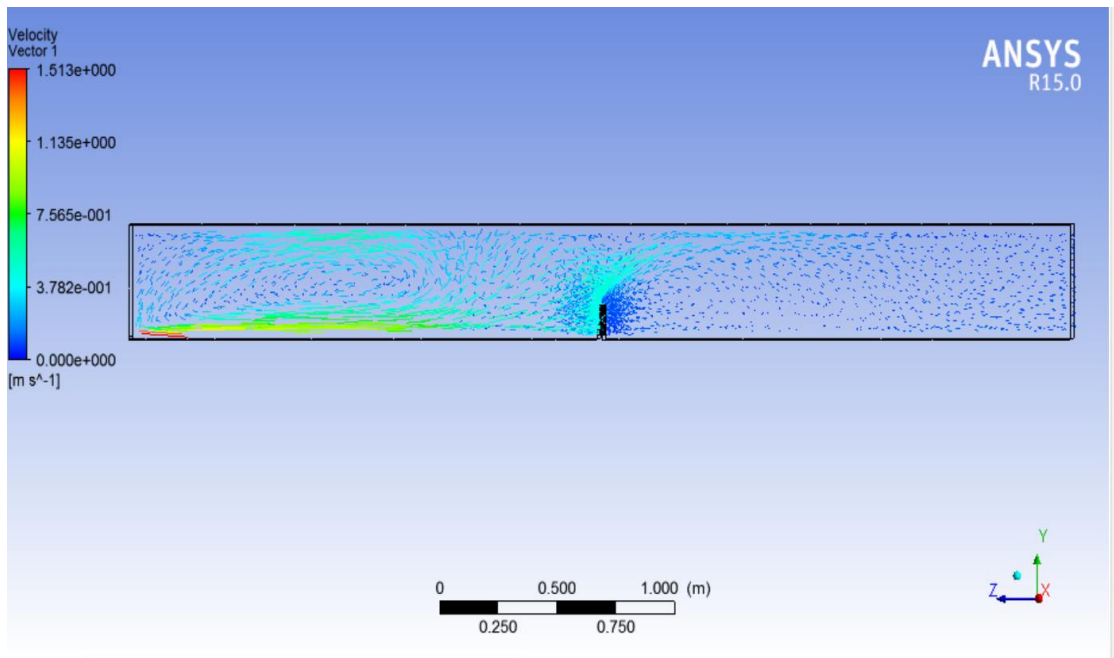


Fig 4.13 hydraulic jump at toe for discharge of $0.0092 \text{ m}^3/\text{s}$

At the discharge (92%) it was found that jump of sufficient intensity are occurring on toe of spillway and length of jump was more and restricted within the span of stilling basin with the help of stepped weir . Hydraulic jump phenomenon became stable after 40 second in ansys fluent.

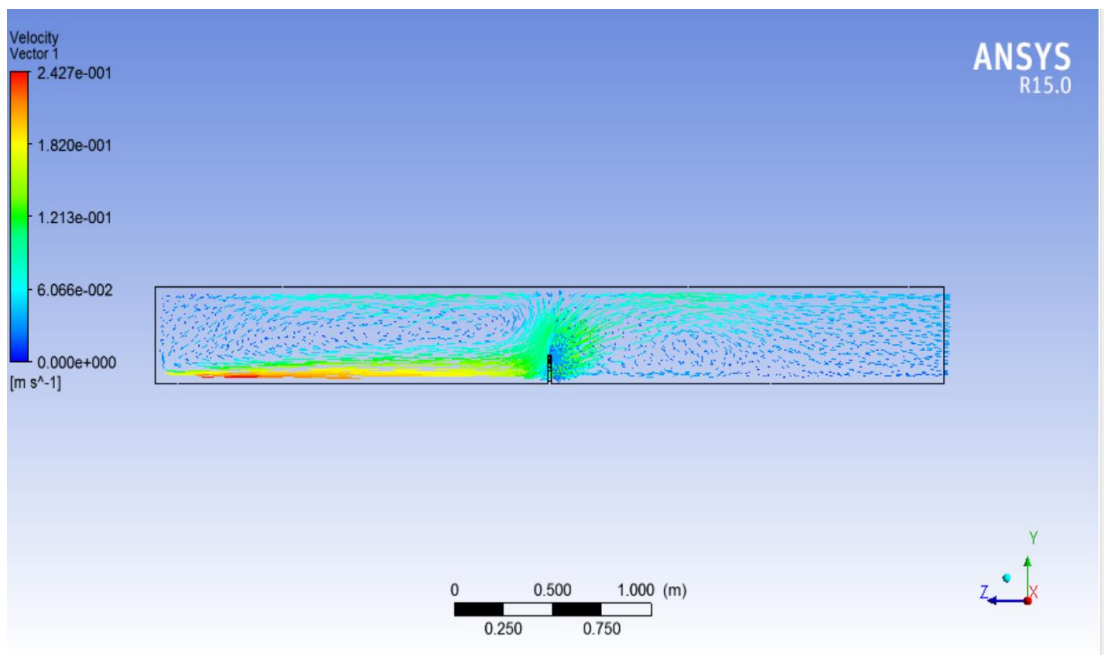


Fig 4.14 Hydraulic jump at toe at discharge of $0.0010 \text{ m}^3/\text{s}$

At the discharge (100%) it was found that jump of strong intensity are occurring on toe of spillway and length of jump was more and restricted within the span of stilling basin with the help of stepped weir . Hydraulic jump phenomenon became stable after 40 second in ansys fluent. It was clearly visible how stepped weir is helping in making jump start location at toe of sluice.

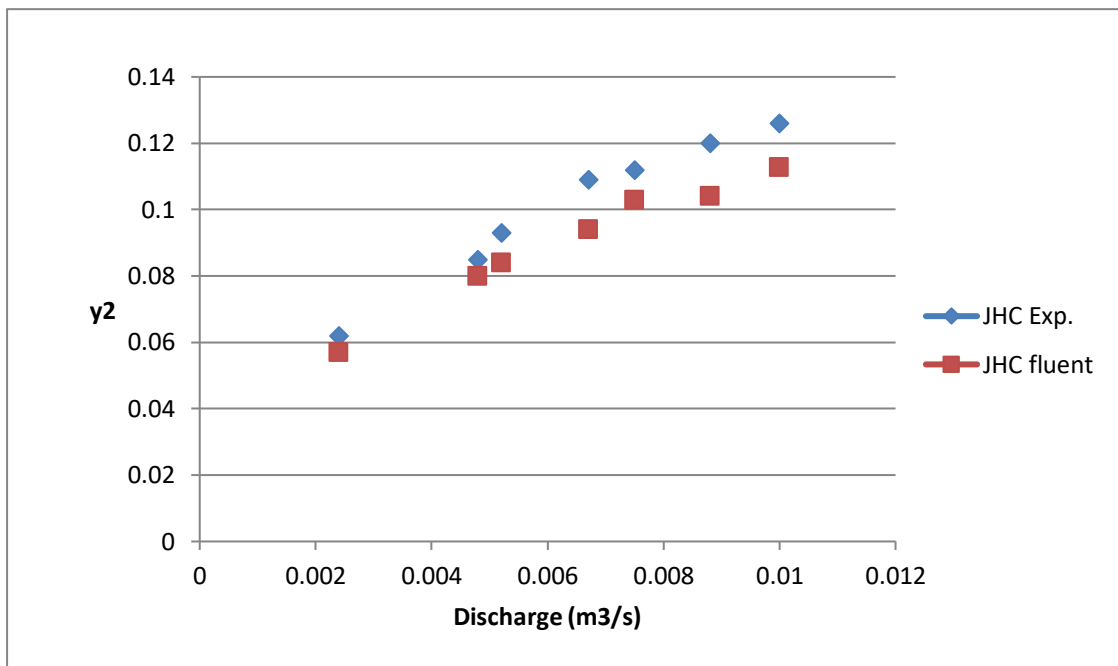


Fig 4.15 Comparison of Experimental and Fluent – JHC (y 2)

for horizontal apron ($C_{dm} = 0.5$)

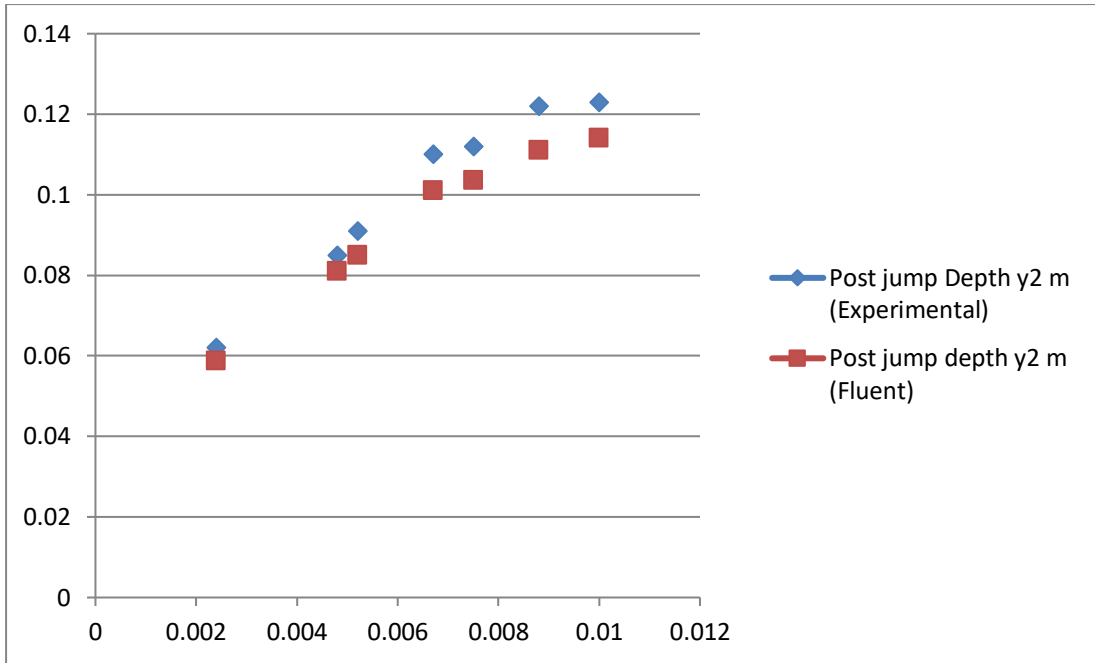


Fig 4.16 Comparison of Experimental and Fluent – JHC (y 2)

for horizontal apron ($C_{dm} = 0.55$)

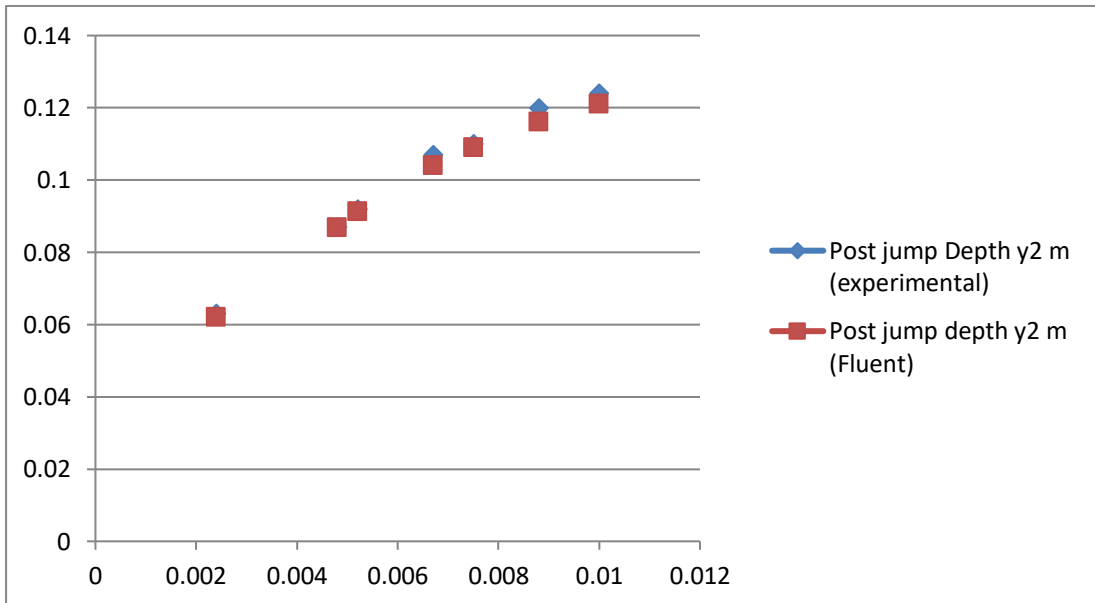


Fig 4.17 Comparison of Experimental and Fluent – JHC (y 2)

for horizontal apron ($C_{dm} = 0.6$)

4.5 Case study of Pawana Dam

A case study of pawana dam is carried out at laboratory scale with the help of existing broad crested weir and proposed broad crested designed weir. The performance of weirs is checked for eight discharges. The domain of problem setup for Pawana dam (prepared in Gambit) is shown in Fig. 4.16. As Fluent is not able to reproduce flow over spillway properly, a sluice gate opening is used to generate supercritical flow. Velocity inlet boundary condition is used at the sluice gate opening.

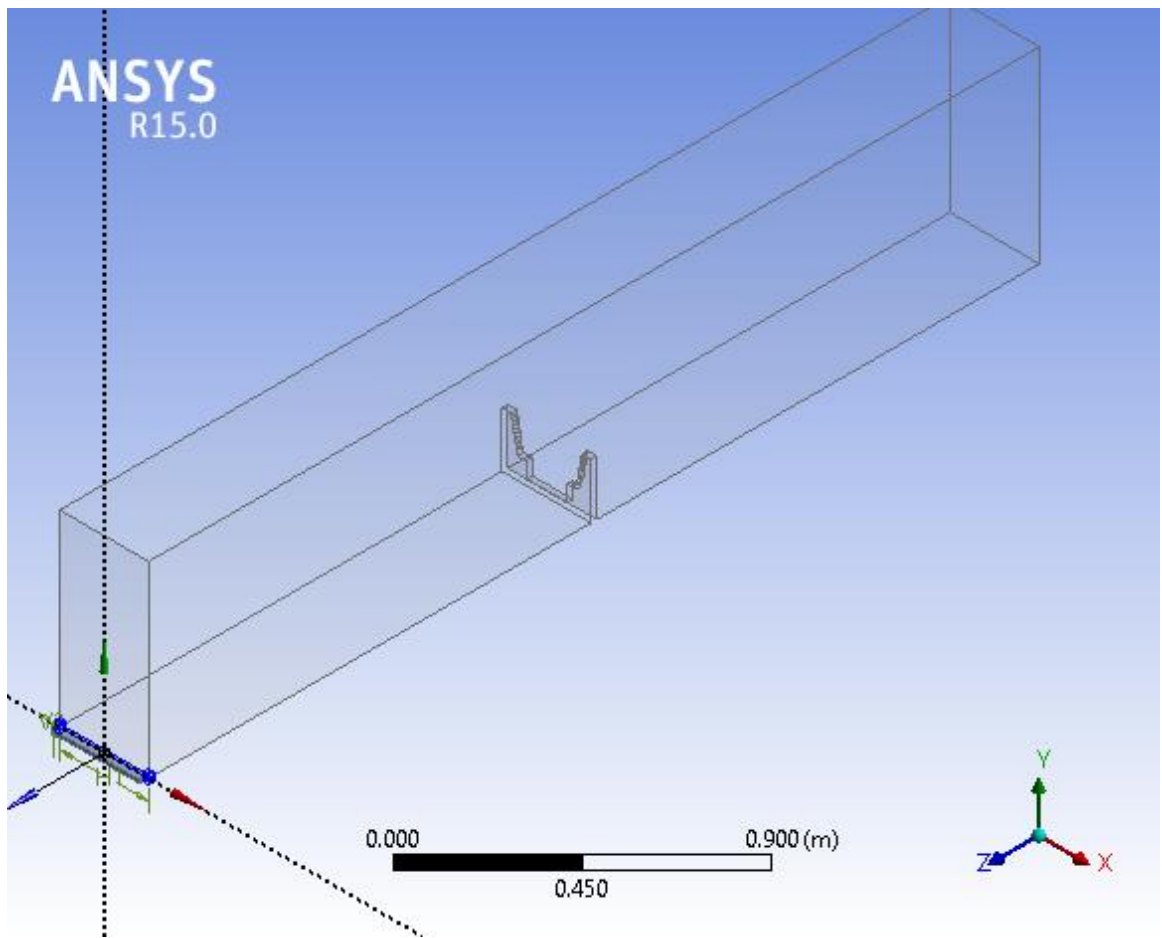


Fig. 4.18 Schematic of problem setup for pawana dam spillway in Gambit

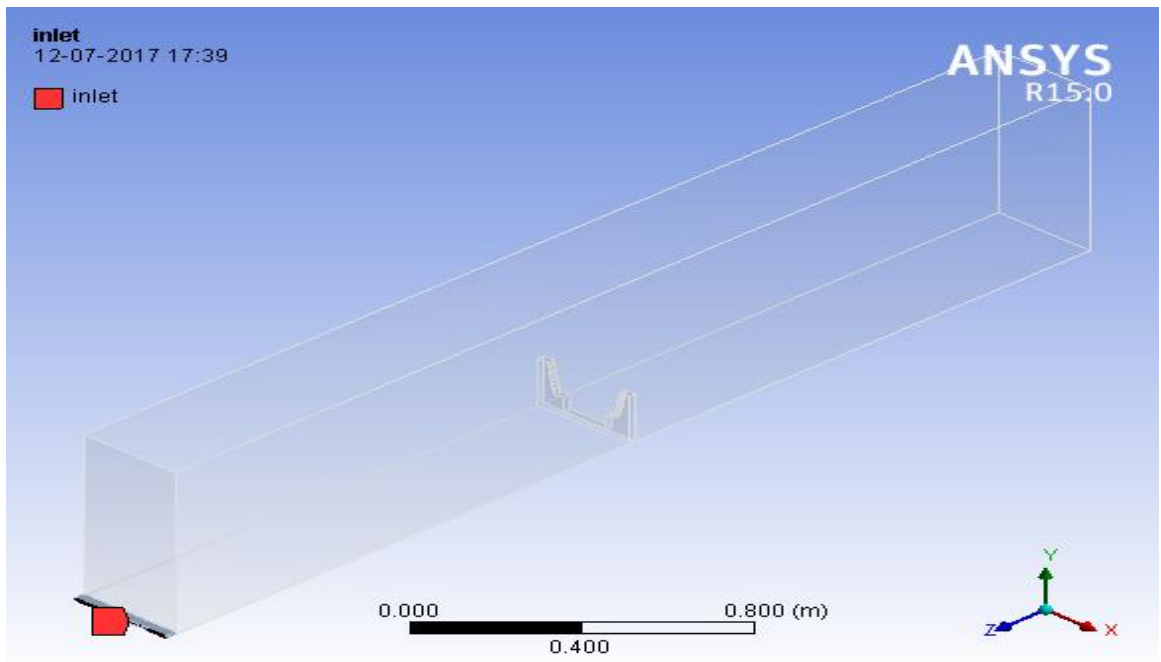


Fig 4.19 inlet section of flume model of pawana dam spillway

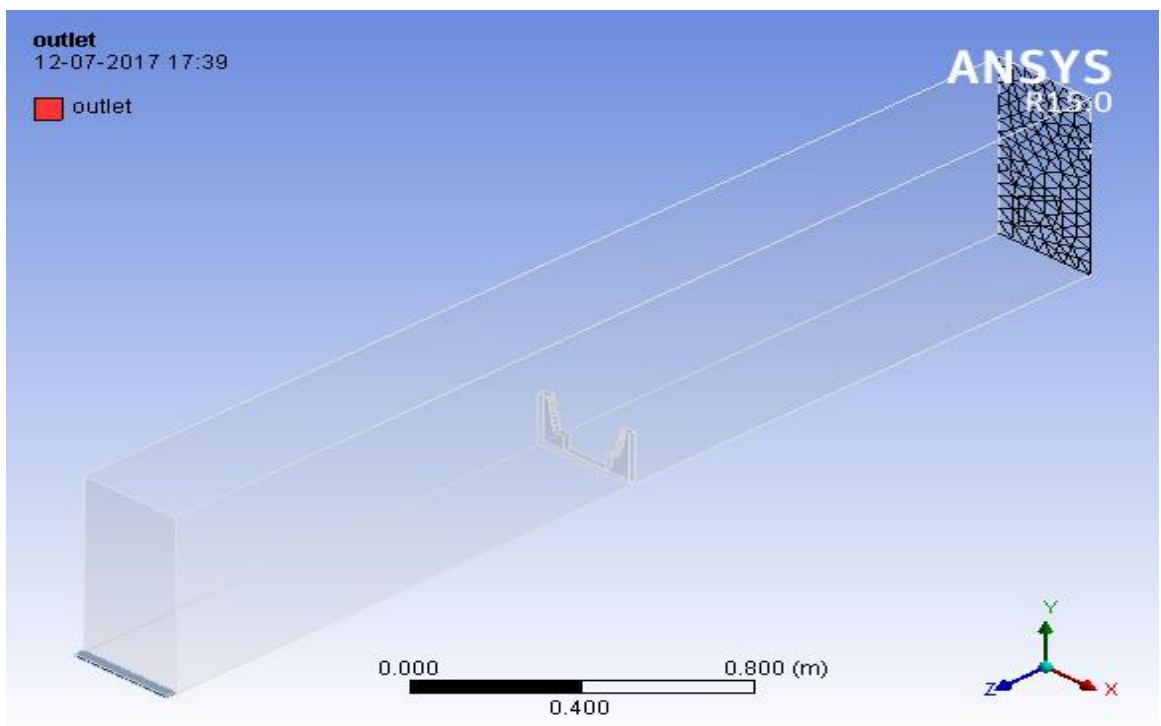


Fig 4.20 Outlet section of flume model of pawana dam spillway

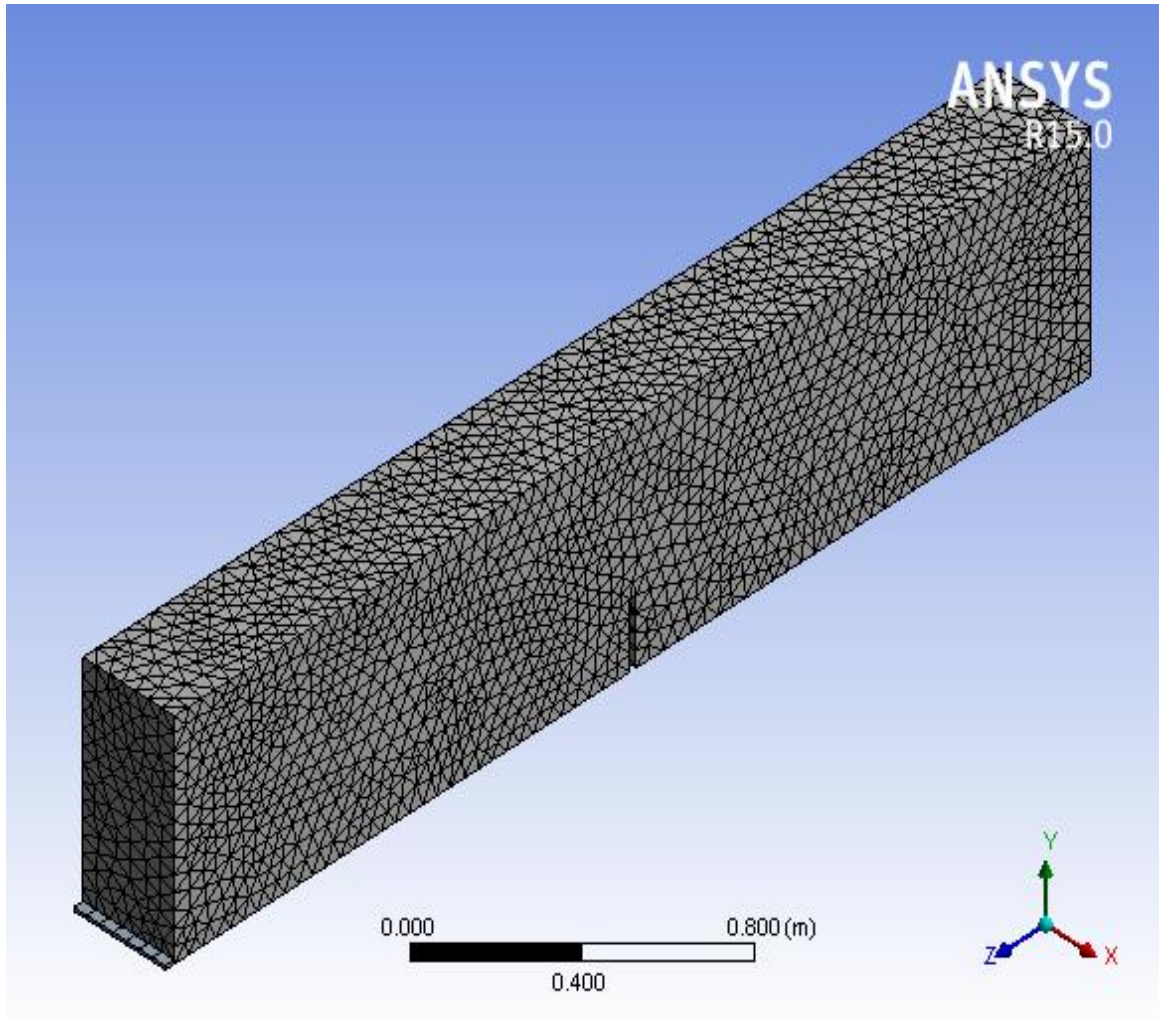


Fig 4.21 Meshed form of flume model of Pawana dam spillway

In all the runs, post jump depths are measured and compared with experimental results. It is found that depths measured on fluent are little bit on higher side than the corresponding experimental depths. Probably this is because; the unit discharge in case of Pawana dam is more.

Table 4.4 Comparison of post jump depths for Pawana dam – experimental and Fluent (designed weir)

Test No.	Discharge Q m ³ /s (Fluent)	Post jump Depth y ₂ m (Expt)	Post jump Depth y ₂ m (Fluent)	Tail water Depth y _t m (Expt)	Tail water depth y _t m (Fluent)	Submergence Ratio S _r (Fluent)
1	0.0200	0.195	0.2070	0.054	0.0627	0.211
2	0.0181	0.186	0.1922	0.052	0.0579	0.202
3	0.0160	0.175	0.1846	0.049	0.0554	0.196
4	0.0130	0.158	0.1640	0.045	0.0484	0.174
5	0.0095	0.135	0.1455	0.04	0.040	0.132
6	0.0077	0.120	0.1260	0.037	0.0343	0.101
7	0.0065	0.110	0.1204	0.035	0.0328	0.091
8	0.0043	0.090	0.1002	0.03	0.03	0.079

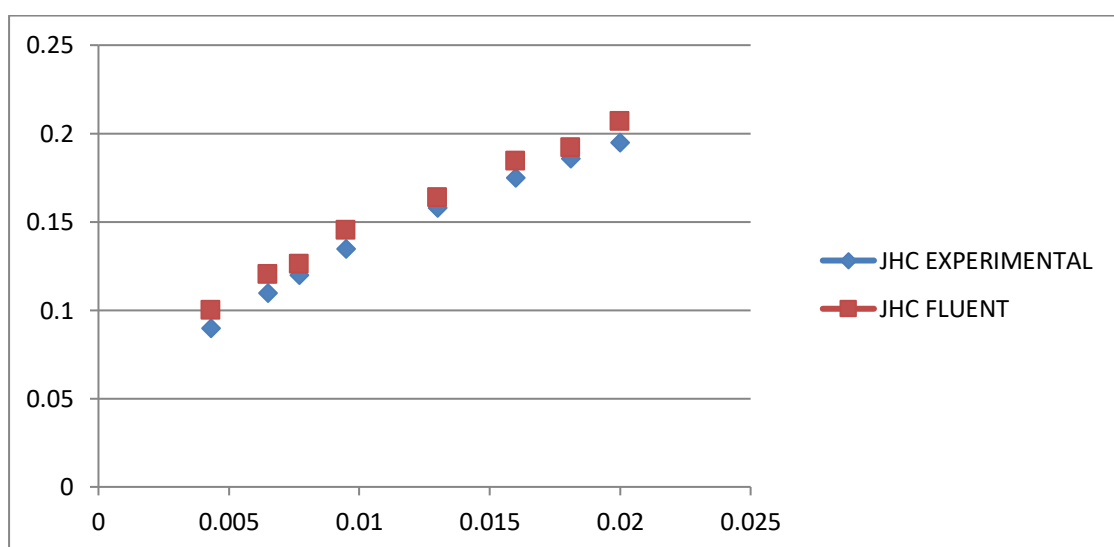


Fig. 4.22 Comparison of Experimental and Fluent – JHC (y₂) for Proposed designed weir

Table 4.5 Comparison of post jump depths for Pawana dam –
experimental and Fluent (existing weir)

<i>Test No.</i>	<i>Discharge Q m³/s (Fluent)</i>	<i>Post jump depth y_2 m (Expt)</i>	<i>Post jump depth y_2 m (Fluent)</i>	<i>Tail water depth y_t m (Expt)</i>	<i>Tail water Depth y_t m (Fluent)</i>
1	0.0200	0.208	0.1996	0.05	0.0346
2	0.0181	0.202	0.1912	0.047	0.0324
3	0.0160	0.195	0.1880	0.044	0.0291
4	0.0130	0.187	0.1780	0.04	0.0234
5	0.0095	0.175	0.1680	0.035	0.0202
6	0.0077	0.163	0.1620	0.03	0.0151
7	0.0065	0.15	0.1540	0.025	0.0104
8	0.0043	0.144	0.1466	0.018	0.0087

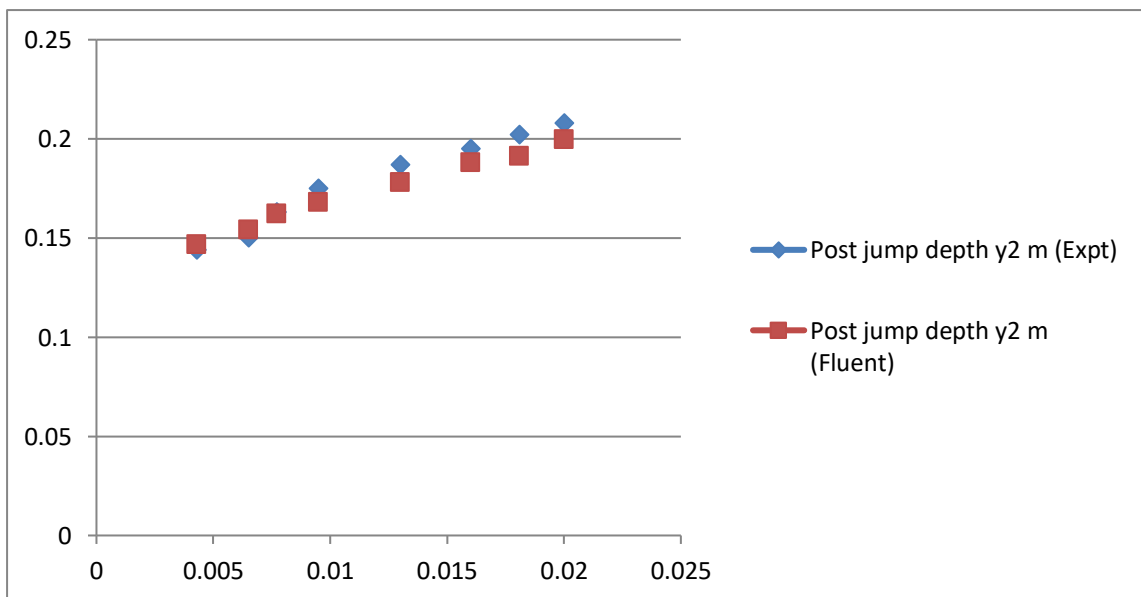


Fig. 4.23 Comparison of Experimental and Fluent - JHC (y_2)
for existing broad crested weir

4.6 Results and Discussions

CFD Studies – Post processing for Horizontal apron cases

In fluent, output can be obtained in various forms. Fig. 4.2 shows geometry of designed weir. It is preferred to have display of results in the form of velocity vectors for the longitudinal and cross sections. To observe the development of hydraulic jump over a period of time, longitudinal sections are taken after every 5 seconds. It also demonstrates the development of hydraulic jump over a period of time. A steady state is obtained after around 35-40 seconds, after which no considerable changes were observed in the pattern.

The discharges are obtained in the 'report' menu in the form of flux. As the inflow and outflow discharge is almost same, the convergence behavior is found to be satisfactory. The post jump depths are directly measured on the contours of volume fraction (water) as shown in the longitudinal sections taken in symmetry after the steady state is reached. Table 4.1, 4.2 and 4.3 show post jump depths, tail water depths and submergence ratio as obtained in Fluent. The post jump depths obtained in Fluent are compared with experimental post jump depths and are found to be on lower side. The post jump depths and tail water depths obtained with Fluent and experiments are plotted in Fig. 4.15, 4.16 and 4.17. Good agreement is found between the experimental and numerical results of post jump depth as the correlation coefficient is around 0.99. In all the tests conducted on Fluent; a clear hydraulic jump has formed at vena contracta of the supercritical flow.

Case Study of Pawana Dam

The simulation of Pawana dam spillway energy dissipator with stepped and existing broad crested weirs is carried out in Fluent. Table 4.4 and Table 4.5 show post jump depths and tail water depths obtained by experiments and Fluent for proposed and existing broad crested weir respectively. The submergence ratios as obtained on Fluent are also given. Fig 4.22 and 4.23 shows comparison of JHC and TWRC between experimental and Fluent results for proposed stepped and existing broad crested weir respectively. In both the cases the JHC (expt.) lie below JHC (Fluent). The TWRC (Fluent) lie above TWRC (expt.) for proposed weir whereas TWRC (Fluent) lie below TWRC (expt.) for existing weir. Again in both the cases the hydraulic jump locations are found to be satisfactory even though in experimental trial with existing weir, the jumps are found to be drowned for all the lower discharges.

4.7 Closure

To validate numerical model - Fluent, CFD studies of cases of horizontal apron are carried out with sharp crested weir. It is found that CFD can predict post jump depths on weir upstream with accuracy. But tail water depths on weir downstream are not satisfactory. CFD could not simulate the accurate location of front of hydraulic jump. Either it has given jumps located near sluice gate or toe of spillway or it has given total sweep out. The intermediate locations of jumps were not captured by CFD. Since post jump depth is an important indicator of the location of jump and predictions of post jump depths is satisfactory, within certain limits CFD simulation is giving satisfactory results.

Chapter 5

Conclusions

A mathematical procedure and computational technique is developed to design geometry of rectangular designed weir. A relation between average S_r and C_{dm} is established empirically. A numerical model Fluent is validated with the help of laboratory data. Performance of designed weir verified with the help of ansys fluent software as the location of front of hydraulic jump is restricted near toe of spillway for different discharges (ranging from Q_{min} to Q_{max} and $F_{r1} > 4.5$) and specific range of S_r . In a nutshell the thesis presents a new design of hydraulic jump type stilling basin for tail water deficiency.

The results of laboratory experiments are used to validate these analysis in Fluent. Though there are certain limitations of CFD towards location of hydraulic jump and tail water submergence, the predictions of post jump depths are satisfactory.

5.1 Practical Applications

To find practical suitability of proposed technique, a pilot scale model study is carried out by considering data of an existing Bhama Askhed dam in India. Following are the findings of the model study.

1. A new stilling basin in the form of horizontal apron with a rectangular broad crested designed weir is designed to carry out pilot scale model study.
2. The performance is checked for four discharges (25%, 50%, 75% and 100% of the design discharge). It is found that for all these discharges clear hydraulic jumps are formed and are located near toe of spillway.

Therefore it is concluded that the proposed mathematical procedure can be used on field to design efficient stilling basins for tail water deficiency conditions.

5.2 Limitations

The present methodology for design of stilling basin has practical significance and proves to improve its intended function. However the following limitations are noted.

1. The mathematical procedure developed in the study is applicable for $F_{r1} > 4.5$ only.
2. There are chances of cavitations in weir due to too many rectangular sharp edges .
3. As the water enters tail channel, due to sudden expansion in open channel, there are chances of separation of flow on either side of the designed weir and is not considered in present case.

5.3 Future Scope

The proposed new design of stilling basin can be made more practicable by overcoming the above limitations. Some of them are discussed in this section.

1. There are chances of cavitations in sharp crested weir on rectangular edge , it Can be made in favourable working condition by using least square Curve method. which will make it workable on real site of dam.
2. Through validation of numerical model Fluent may be done covering satisfactory results for length and location of jump. Then it can be used as an alternative to costly and time consuming physical model studies for experimental verification.
3. Hydraulic jumps on different sloping aprons may be studied in depth to explore the suitability of present technique.

References

1. Achour, B., Debabeche, M. (2003). "Control of hydraulic jump by sill in triangular channel". J. Hydr. Res., 41(3), 319-325.
2. Alhamid (2004). "Jump characteristics on sloping basins". J. Hydr. Res., 42(6), 657-662.
3. Anderson, J.D. (1995). "Computational fluid dynamics". McGraw-Hill book company, Inc., New York, 1995.
4. Bhowmik, N.G. (1975). "Stilling basin design for low Froude number". J. Hydr. Engg., ASCE, 101(7), 901-915.
5. Bowers, C.E., Toso, J. (1988). "Karnafuli project, model studies of spillway damage". J.Hydr.Engg., ASCE, 114(5), 469-483.
6. Cassidy, J.J. (1990). "Fluid mechanics and design of hydraulic structures". J.Hydr.Engg., ASCE, 116(8), 961-977.
7. Chaudhry, Z.A. (2008). "Energy dissipation problems downstream of Jinnah barrage". Pak. J. Engg. & Appl. Sci., 3 (7), 19-25.
8. Chippada, S., Ramaswami, B., Wheeler, M.F. (1994). "Numerical simulation of hydraulic jump". Journal for Numerical Methods in Engg., 37(8), 1381-1397.
9. Chow, V.T. (1959). "Open channel hydraulics". McGraw-Hill book company, Inc., New York, 1959.
10. Christopher, B.C., Marshall, C. R. (2001). "Simulation of tailrace hydrodynamics using computational fluid dynamics models". Report No. PN NL-13467, USACE.

11. Design of small dams (1974). "Chapter IX-Spillways" . A water resources technical publication, U.S. Bureau of Reclamation.
12. Forster, J.W., Skrinde, R.A. (1950). "Control of the hydraulic jump by sills". *Trans. ASCE*, 115, 973-1022.
13. Gogus, M., Defne, Z., Ozkandemir, V. (2006). "Broad -crested weirs with compound cross sections". *J. Irrigation and Drainage Engg., ASCE*, 132(3), 272-280.
14. Govinda Rao N.S., Rajaratnam, N. (1963). "The submerged hydraulic jump". *J.Hydr.Engg.,ASCE*, 89 (1), 139-162.
15. Gunal, M, Narayanan, R. (1996). "Hydraulic jump in sloping channel". *J. Hydr. Engg., ASCE*, 122(8), 436-442.
16. Hinge G. A., Balkrishna S., Khare K.C. (2010), Pawana Dam Energy Dissipation – A Case Study, *Australian Journal of Basin and Applied Sciences*, Vol.4(8), pp. 3261-3267.
17. Hinge G. A., Balkrishna S., Khare K.C. (2010), Improved Design of Stilling Basin for Deficient Tail Water, *Journal of Basic and Applied Scientific Research*, Vol.1(1), pp. 31-40.
18. Rajaratnam, N., Subramanya, K. (1966). "Profile of the hydraulic jump". *J. Hydr. Engg., ASCE*, 94(3), 663-672.
19. Rouse, H., Siao, T.T., Nagaratnam, S. (1958). "Turb ulence characteristics of the hydraulic jump". *J. Hydr. Engg., ASCE*, 84(1), Proc. Paper, 1528-1-31.
20. Subramanya, K. (1986). "Flow in open channels". Tat a McGraw-Hill Publishing Co. Ltd., New Delhi, India.
21. Swamee, P.K. (1988). "Generalized rectangular weir equations". *J. Hydr. Engg., ASCE*, 114(8), 945-949.

22. Tu, J., Yeoh, G.H., Liu, C. (2008). "Computational Fluid Dynamics", Chapter 6, Elsevier Publication.
23. Tung, Y.K., Mays, L.W. (1982). "Optimal design of stilling basins for overflow spillway". J. Hydr. Engg., ASCE, 108(10), 1163-1178.
24. Vittal, N., Al-Garni, A.M. (1992). "Modified type III stilling basin – new method of design". J. Hydr. Res., 30(4), 485-498.

